*Journal of Molecular Structure*, 193 (1989) 1-34
Elsevier Science Publishers B.V., Amsterdam — Printed in The Netherlands


# AB INITIO FORCE FIELDS OF GLYCINE DIPEPTIDE IN $C_5$ AND $C_7$ CONFORMATIONS

T.C. CHEAM and S. KRIMM

*Biophysics Research Division and Department of Physics, University of Michigan, Ann Arbor, Michigan 48109 (U.S.A.)*

(Received 14 March 1988)

## ABSTRACT

Schäfer and coworkers have previously derived, with the 4-21 Gaussian basis set, ab initio optimized geometries for the glycine dipeptide, $CH_3CONHCH_2CONHCH_3$, in several conformations. Using their geometries for the $C_5$ and $C_7$ conformations, respectively with five- and seven-membered intramolecular NH···OC hydrogen-bonded rings, we have computed the vibrational force fields and dipole moment derivatives at the 4-21 level. Scale factors for the quadratic force constants were transferred, with two changes, from the set derived by Fogarasi and Balázs from a study of small amides. The differences in the force constants, harmonic frequencies, dipole derivatives, and infrared intensities between the conformations and within each conformation are discussed and related, where possible, to differences in hydrogen bonding and structure. In particular, the NH and CO stretch and bend force constants and dipole derivatives show trends that can be correlated with the $C_5$ and $C_7$ hydrogen bonds. The amide modes are compared with some available data on glycine dipeptide in argon matrix, and the comparison supports the empirically-based conclusion that $C_5$ and $C_7$ conformations are both present in the matrix-isolated sample.

## INTRODUCTION

The dipeptide model has been much used to study the intramolecular interactions that help to determine the conformations of polypeptides and proteins [1]. Schäfer and coworkers [2,3] have derived, with the 4-21 basis set, ab initio energy-gradient optimized geometries for the glycine dipeptide, $CH_3CONHCH_2CONHCH_3$, in several conformations. Using their geometries for the two lowest energy conformations, $C_5$ and $C_7$, respectively with five- and seven-membered intramolecular NH···OC hydrogen-bonded rings, we have computed the vibrational force fields and dipole moment derivatives at the 4-21 level. To correct for systematic errors in the force constants due to neglect of electron correlation and to finite basis set size [4], we have transferred, with minor changes, the 4-21 scale factors found by Fogarasi and Balázs from a study of small amides [5].

The force field of the peptide group in *N*-methylacetamide has been com-

0022-2860/89/$03.50 

puted at the 4-31G and 4-31G* levels by Sugawara et al. [6,7] and at the 4-21 level by Balázs [8]; and in recent ab initio [9] and experimental [10] work, we studied the sensitivity of the peptide group modes to intermolecular hydrogen bonding. The dipeptide model allows study of the effects of conformation as well as intramolecular hydrogen bonding on the force field and normal modes of the peptide group. In previous vibrational analyses of polypeptides [11], a standard geometry was assumed for the peptide unit in all conformations. Force constants were either transferred unchanged between conformations, so that frequency shifts resulted only from dihedral angle changes; or reasonable but quite arbitrary adjustments were made, in which case the effects of geometry variations were incorporated into the force constants, reducing their transferability and physical meaningfulness. Schäfer and coworkers [2,3,12] have clearly shown the necessity of allowing bond lengths and angles in peptides to vary with conformation. Quantum mechanical calculations of the force fields of optimized dipeptide conformations should help in the development of more effective force fields for normal mode calculations of polypeptides and proteins, and in parameterizing more accurate molecular mechanics energy functions [13] for studying structure and dynamics. We previously also calculated infrared intensities of the amide modes in *N*-methylacetamide and polyglycine I using ab initio dipole moment derivatives for the CONH group in *N*-methylacetamide [14]. Dipeptides allow determination of group moment derivatives for side chains, and will also allow study of the conformational dependence of group moment derivatives and their transferability.

In numerous infrared studies, $C_5$ and $C_7$ conformations have been proposed for glycine dipeptide in dilute solution [15–20] and in argon matrix [21], and crystalline glycine dipeptide has also been investigated [22,23]. Other than the NH stretches, the assignments of bands to $C_5$ and $C_7$ conformations are not conclusive or complete. In the following, after giving details of our calculations, we discuss the theoretical force fields, frequencies and dipole derivatives, and then compare our results with available experimental data.

## METHOD OF CALCULATION

The $C_5$ and $C_7$ structures are shown in Fig. 1; the Cartesian axes and atomic coordinates are as given by Schäfer et al. [2]. The $C_5$ conformation (GLY5) has dihedral angles [24] $(\phi,\psi) = (180°,180°)$ and is a fully extended chain with planar symmetry, and the $C_7$ conformation (GLY7) has $(\phi,\psi) = (83.4°,-70.7°)$. The $C_7$ $\phi$ and $\psi$ values are those in which an L-residue would be axial to the seven-membered hydrogen-bonded ring; an equal-energy $C_7$ equatorial conformation with $(\phi,\psi) = (-83.4°,70.7°)$ has also been derived by Klimkowski et al. [3]. We have not applied empirical corrections to the ab initio geometries; such corrections have been recommended [4] in view of the dependence of ab initio force constants on the reference geometry used.

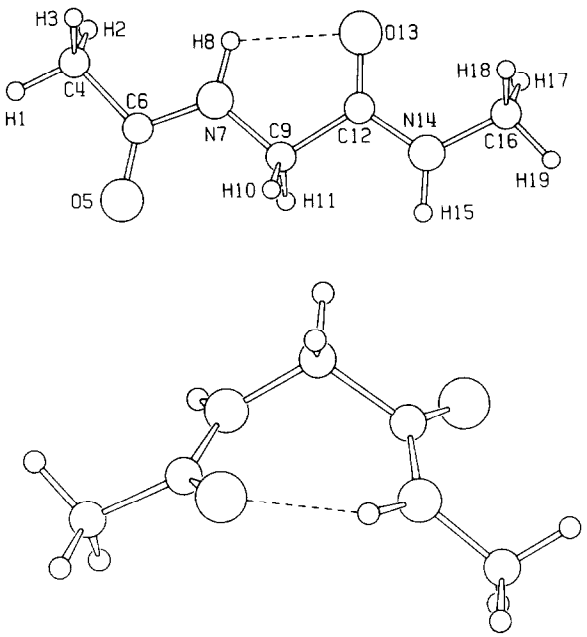


Fig. 1. Glycine dipeptide $C_5$ (top) and $C_7$ (bottom) conformations.

Our aim is mainly to study the force field changes between the two conformations; moreover, the corrections for peptides may not be as reliably known, particularly in the presence of hydrogen bonding.

The quadratic and semi-diagonal cubic force constants were computed from the analytical energy gradient using two-sided displacements along internal coordinates; dipole moment derivatives were also evaluated [25,26]. The primitive internal coordinates $\vec{\mathbf{R}}$ are listed in Table 1; the out-of-plane bends and torsions are defined as in ref. 27. The group, or local symmetry, coordinates [28] $\vec{\mathbf{S}}$ are defined in Table 2. Cartesian displacements corresponding to each $S_i$ were obtained by [29] $\vec{\mathbf{X}} = \mathbf{M}^{-1}\tilde{\mathbf{B}}(\mathbf{B}\mathbf{M}^{-1}\tilde{\mathbf{B}})^{-1}\vec{\mathbf{S}}$ where $\mathbf{M}$ is the diagonal matrix of atomic masses and $\mathbf{B}$ is defined by $\vec{\mathbf{S}} = \mathbf{B}\vec{\mathbf{X}}$. Bond lengths were displaced by $\pm 0.01$ Å, and out-of-plane bends and torsions by $\pm 0.025$ rad (the actual changes in out-of-plane angles are then $\pm 0.025/\sin\alpha$ rad, where $\alpha$ is the angle opposite the bond involved [27,28]). For the bond angle bends each $\Delta S_i$ was chosen such that the maximum angular distortions were $\pm 0.025$ rad; the relation is $\Delta S_i = \pm 0.025/U_{\text{im}}$, where $U_{\text{im}}$ is the largest normalized coefficient in $S_i$. The group coordinates are consistent with the recommendations of Pulay et al. [25] except for $NC^{\alpha}C$ def and $CH_2$ bend. The wide occurrence of characteristic group frequencies ensures that the off-diagonal force constants in such a coordinate basis will be small [25,28].

In using these group coordinates in force field and normal mode calculations

TABLE 1

Internal coordinates for glycine dipeptide

| *R* | Atoms | GLY5[a] | GLY7[a] | *R* | Atoms | GLY5[a] | GLY7[a] |
|---|---|---|---|---|---|---|---|
| *Bond stretches* | | | | | | | |
| 1 | 4-6 | 1.517 | 1.516 | 32 | 6-4-2 | 110.3 | 110.1 |
| 2 | 6-7 | 1.354 | 1.354 | 33 | 6-4-3 | 110.3 | 110.4 |
| 3 | 7-9 | 1.447 | 1.467 | 34 | 1-4-2 | 109.6 | 109.5 |
| 4 | 6-5 | 1.225 | 1.229 | 35 | 1-4-3 | 109.6 | 109.7 |
| 5 | 7-8 | 0.996 | 0.994 | 36 | 2-4-3 | 108.4 | 108.6 |
| 6 | 9-12 | 1.524 | 1.533 | 37 | 7-9-12 | 108.1 | 111.9 |
| 7 | 12-14 | 1.348 | 1.346 | 38 | 7-9-10 | 111.0 | 108.9 |
| 8 | 14-16 | 1.466 | 1.462 | 39 | 7-9-11 | 111.0 | 108.4 |
| 9 | 12-13 | 1.225 | 1.224 | 40 | 12-9-10 | 109.7 | 107.5 |
| 10 | 14-15 | 0.993 | 0.998 | 41 | 12-9-11 | 109.7 | 110.0 |
| 11 | 4-1 | 1.077 | 1.077 | 42 | 10-9-11 | 107.4 | 110.1 |
| 12 | 4-2 | 1.083 | 1.083 | 43 | 14-16-17 | 110.4 | 111.0 |
| 13 | 4-3 | 1.083 | 1.082 | 44 | 14-16-18 | 110.4 | 110.3 |
| 14 | 9-10 | 1.083 | 1.076 | 45 | 14-16-19 | 108.6 | 108.6 |
| 15 | 9-11 | 1.083 | 1.079 | 46 | 17-16-18 | 108.6 | 108.2 |
| 16 | 16-17 | 1.080 | 1.082 | 47 | 17-16-19 | 109.4 | 109.3 |
| 17 | 16-18 | 1.080 | 1.081 | 48 | 18-16-19 | 109.4 | 109.3 |
| 18 | 16-19 | 1.079 | 1.079 | | | | |
| *Angle bends* | | | | *Out-of-plane bends*[b] | | | |
| 19 | 4-6-7 | 115.0 | 115.1 | 49 | 6-5 | 0.0 | 0.1 |
| 20 | 4-6-5 | 123.4 | 122.9 | 50 | 7-8 | 0.0 | −2.0 |
| 21 | 7-6-5 | 121.5 | 122.0 | 51 | 12-13 | 0.0 | −0.1 |
| 22 | 6-7-9 | 120.1 | 121.6 | 52 | 14-15 | 0.0 | 4.1 |
| 23 | 6-7-8 | 123.9 | 120.2 | | | | |
| 24 | 9-7-8 | 116.0 | 118.2 | *Torsions* | | | |
| 25 | 9-12-14 | 115.1 | 114.3 | 53 | 4-6 | | |
| 26 | 9-12-13 | 122.0 | 121.8 | 54 | 6-7 | | |
| 27 | 14-12-13 | 123.0 | 123.8 | 55 | 7-9 | | |
| 28 | 12-14-16 | 120.5 | 120.2 | 56 | 9-12 | | |
| 29 | 12-14-15 | 120.3 | 119.0 | 57 | 12-14 | | |
| 30 | 16-14-15 | 119.2 | 120.7 | 58 | 14-16 | | |
| 31 | 6-4-1 | 108.6 | 108.6 | | | | |

[a]Equilibrium values: bond lengths in Å, angles in degrees.
[b]Positive: $C_6$, $N_{14}$ move out of GLY5 plane in Fig. 1; $N_7$, $C_{12}$ move below plane.

of ab initio rather than ideal [11] structures, some approximations are involved. The group angle bend coordinates are strictly appropriate only if the branching redundancies at the backbone atoms are the simple sums of the primitive angle bends. For the $sp^3$ carbons, the angles are not tetrahedral and the coefficients in the redundancy relations are no longer unity [30]. Also, in GLY5 the bonds at the C and N atoms are coplanar and the branching redun-

TABLE 2

Group coordinates for glycine dipeptide[a]

| | | | | | |
|---|---|---|---|---|---|
| $S_1 = R_5$ | NH str1 | $S_{27} = R_{34}+R_{35}+R_{36}-R_{31}-R_{32}-R_{33}$ | M1 sb |
| $S_2 = R_4$ | CO str1 | $S_{28} = 2R_{36}-R_{34}-R_{35}$ | M1 ab1 |
| $S_3 = R_2$ | CN str1 | $S_{29} = R_{34}-R_{35}$ | M1 ab2 |
| $S_4 = R_1$ | MC str | $S_{30} = 2R_{31}-R_{32}-R_{33}$ | M1 rock1 |
| $S_5 = R_3$ | $NC^{\alpha}$ str | $S_{31} = R_{32}-R_{33}$ | M1 rock 2 |
| $S_6 = R_{10}$ | NH str2 | $S_{32} = 5R_{37}-R_{38}-R_{39}-R_{40}-R_{41}-R_{42}$ | $NC^{\alpha}C$ def |
| $S_7 = R_9$ | CO str2 | $S_{33} = 4R_{42}-R_{38}-R_{39}-R_{40}-R_{41}$ | $CH_2$ bend |
| $S_8 = R_7$ | CN str2 | $S_{34} = R_{38}+R_{39}-R_{40}-R_{41}$ | $CH_2$ wag |
| $S_9 = R_6$ | $C^{\alpha}C$ str | $S_{35} = R_{38}-R_{39}-R_{40}+R_{41}$ | $CH_2$ twist |
| $S_{10} = R_8$ | NM str | $S_{36} = R_{38}-R_{39}+R_{40}-R_{41}$ | $CH_2$ rock |
| $S_{11} = R_{11}$ | MH1 str | $S_{37} = R_{46}+R_{47}+R_{48}-R_{43}-R_{44}-R_{45}$ | M2 sb |
| $S_{12} = R_{12}$ | MH2 str | $S_{38} = 2R_{46}-R_{47}-R_{48}$ | M2 ab1 |
| $S_{13} = R_{13}$ | MH3 str | $S_{39} = R_{47}-R_{48}$ | M2 ab2 |
| $S_{14} = R_{14}$ | CH10 str | $S_{40} = 2R_{45}-R_{43}-R_{44}$ | M2 rock1 |
| $S_{15} = R_{15}$ | CH11 str | $S_{41} = R_{43}-R_{44}$ | M2 rock2 |
| $S_{16} = R_{18}$ | MH19 str | $S_{42} = R_{49}\sin(4\text{-}6\text{-}7)$ | CO ob1 |
| $S_{17} = R_{16}$ | MH17 str | $S_{43} = R_{50}\sin(6\text{-}7\text{-}9)$ | NH ob1 |
| $S_{18} = R_{17}$ | MH18 str | $S_{44} = R_{51}\sin(9\text{-}12\text{-}14)$ | CO ob2 |
| $S_{19} = 2R_{19}-R_{20}-R_{21}$ | MCN def | $S_{45} = R_{52}\sin(12\text{-}14\text{-}16)$ | NH ob2 |
| $S_{20} = R_{20}-R_{21}$ | CO ib1 | $S_{46} = R_{53}$ | MC tor |
| $S_{21} = 2R_{22}-R_{23}-R_{24}$ | $CNC^{\alpha}$ def | $S_{47} = R_{54}$ | CN tor1 |
| $S_{22} = R_{23}-R_{24}$ | NH ib1 | $S_{48} = R_{55}$ | $NC^{\alpha}$ tor |
| $S_{23} = 2R_{25}-R_{26}-R_{27}$ | $C^{\alpha}CN$ def | $S_{49} = R_{56}$ | $C^{\alpha}C$ tor |
| $S_{24} = R_{26}-R_{27}$ | CO ib2 | $S_{50} = R_{57}$ | CN tor2 |
| $S_{25} = 2R_{28}-R_{29}-R_{30}$ | CNM def | $S_{51} = R_{58}$ | NM tor |
| $S_{26} = R_{29}-R_{30}$ | NH ib2 | | |

[a]All coordinates normalized. Normalization factors not shown for $S_{19}-S_{41}$.

dancy at each of these atoms is given by the sum of the three in-plane primitive angle bends [30]. In GLY7, however, the bonds are not exactly coplanar, as shown by the equilibrium out-of-plane angles (Table 1). The C and N redundancies in GLY7 are then more complex and will involve the out-of-plane bend coordinates as well. Properly, then, non-redundant group coordinates should be constructed to be orthogonal to the exact redundancies [28,31]. To facilitate comparisons of force constants and dipole derivatives between the two conformations and within each conformation, as well as with other ab initio and empirical force fields, we have used group coordinates orthogonal to the ideal redundancies. (The exact redundancies can be found numerically by diagonalizing the $\mathbf{BM}^{-1}\tilde{\mathbf{B}}$ matrix [32], and non-redundant orthonormal coordinates constructed by the Schmidt process [33]. For GLY5 and GLY7 these coordinates were found to be of the form $aS_i+b\sum$ where $\sum$ is the ideal redundancy. The coefficient $a$ differs from unity by less than $10^{-4}$ for all $S_i$ except $S_{45}$ in GLY7 where it is 0.9985 and where $b$ is largest, $-0.0549$.) As another

approximation, in GLY7 the **B** matrix elements for the out-of-plane bends have been computed assuming strict planarity at the C and N atoms [34].

For the ab initio calculations we used a version of the GAUSSIAN 76 program [35], augmented by an analytical energy gradient link [36]. The 4-21 Gaussian basis is described in ref. 25. As a practical note, the GLY7 runs consumed a total CPU time of 4 weeks on a MicroVAX II, and the GLY5 runs took a total of 17 hours on an IBM 3090-200 running MTS.

We initially scaled our quadratic force constants using the procedure of Fogarasi and Balázs, including their values of the 4-21 scale factors determined from a study of small amides [5]. While most frequencies were reasonable, based on the known characteristic modes of the peptide, methylene and methyl groups, the CH deformation modes were obviously far too high, resulting, in particular, in extraneous mixings with CN stretch and NH in-plane bend in the 1500 $cm^{-1}$ region. We therefore reduced the CH deformation scale factor, yielding purer methyl and methylene modes at more reasonable frequencies. Also, the CH and NH stretch modes were about 150 $cm^{-1}$ higher than expected; since these modes are well localized it was easy to adjust their scale factor too. The final values of the six scale factors are (with Fogarasi and Balázs' values in parentheses, if different): hydrogen stretches, 0.80 (0.88); all other stretches, 0.88; NH bends and $S_{32}$, 0.86; CH bends, 0.76 (0.86); skeletal and CO bends, 0.80; out-of-plane bends and torsions, 0.77. Our reduced CH bend factor is similar to those optimized by Boggs and coworkers for the methyl group in toluene [37], 0.765, and in 1-methyluracil [38], 0.790. One probable reason we had to modify the scale factors for hydrogen stretching and bending coordinates is that unlike Fogarasi and Balázs we did not apply empirical corrections to the ab initio structures. It is possible, of course, that the number of distinct scale factors can be even larger, but we do not have the experimental data needed to determine more parameters. As with the refinement of empirical force fields for large molecules [39], the choice of a set of scale factors and a scaling procedure is not unique.

## FORCE FIELDS AND FREQUENCIES

Because of the large dimension of the **F** matrices for GLY5 and GLY7, we report only the scaled force constants with magnitude $\geqslant 0.01$. All such off-diagonal terms are listed in Table 3, and the diagonal terms, together with off-diagonal elements with magnitude of at least 0.1, are shown in Table 4. The latter table contains a more manageable number of terms and will, for the most part, be the basis of our discussion. In these tables, those $|F_{ij}| < 0.01$ are shown as 0.0; all in-plane/out-of-plane cross terms for GLY5 are, of course, zero by symmetry. Table 5 lists the unscaled diagonal cubic force constants. Finally, Table 6 shows the harmonic frequencies for GLY5 and GLY7 calculated with the scaled force constants in Tables 3 and 4. The frequencies for GLY5 and

TABLE 3

Scaled off-diagonal force constants $|F_{ij}| \geq 0.01$[a]

| Term | GLY5 | GLY7 | Term | GLY5 | GLY7 | Term | GLY5 | GLY7 |
|---|---|---|---|---|---|---|---|---|
| 1-2 | 0.02 | −0.02 | 2-35 | 0.0 | −0.01 | 4-13 | 0.02 | 0.02 |
| 1-3 | −0.05 | −0.01 | 2-36 | 0.0 | −0.07 | 4-14 | 0.0 | 0.02 |
| 1-5 | 0.12 | 0.0 | 2-43 | 0.0 | 0.01 | 4-15 | 0.0 | −0.01 |
| 1-6 | 0.01 | 0.0 | 2-44 | 0.0 | 0.01 | 4-19 | 0.20 | 0.21 |
| 1-7 | −0.09 | 0.0 | 2-45 | 0.0 | −0.01 | 4-20 | 0.24 | 0.25 |
| 1-8 | 0.05 | 0.0 | 2-47 | 0.0 | −0.02 | 4-21 | 0.02 | 0.0 |
| 1-9 | −0.05 | −0.02 | 2-48 | 0.0 | 0.04 | 4-22 | 0.01 | 0.02 |
| 1-11 | −0.01 | −0.01 | 2-49 | 0.0 | −0.05 | 4-23 | 0.0 | −0.01 |
| 1-12 | 0.0 | 0.02 | 2-50 | 0.0 | −0.02 | 4-27 | −0.29 | −0.30 |
| 1-13 | 0.0 | 0.01 | 3-4 | 0.30 | 0.30 | 4-28 | −0.02 | −0.02 |
| 1-14 | 0.0 | 0.02 | 3-5 | 0.15 | 0.24 | 4-30 | 0.03 | 0.04 |
| 1-15 | 0.0 | −0.02 | 3-6 | 0.0 | 0.05 | 4-32 | 0.02 | 0.0 |
| 1-19 | 0.0 | −0.05 | 3-7 | −0.01 | −0.02 | 4-36 | 0.0 | 0.02 |
| 1-20 | 0.0 | −0.03 | 3-8 | −0.02 | −0.10 | 4-47 | 0.0 | −0.02 |
| 1-21 | −0.11 | −0.09 | 3-9 | −0.03 | 0.04 | 4-48 | 0.0 | −0.03 |
| 1-22 | −0.11 | 0.02 | 3-12 | 0.01 | 0.01 | 5-6 | 0.0 | −0.02 |
| 1-24 | −0.02 | 0.0 | 3-13 | 0.01 | 0.01 | 5-7 | 0.04 | 0.10 |
| 1-34 | 0.01 | 0.0 | 3-14 | −0.04 | −0.02 | 5-8 | −0.02 | 0.07 |
| 1-35 | 0.0 | −0.02 | 3-15 | −0.04 | −0.05 | 5-9 | 0.12 | 0.31 |
| 1-36 | 0.0 | −0.02 | 3-19 | 0.17 | 0.15 | 5-14 | 0.13 | 0.05 |
| 1-43 | 0.0 | 0.03 | 3-20 | −0.42 | −0.49 | 5-15 | 0.13 | 0.09 |
| 2-3 | 1.35 | 1.35 | 3-21 | 0.18 | 0.21 | 5-19 | 0.06 | 0.0 |
| 2-4 | 0.36 | 0.35 | 3-22 | 0.17 | 0.20 | 5-20 | 0.10 | 0.0 |
| 2-5 | −0.08 | −0.07 | 3-23 | 0.0 | 0.02 | 5-21 | 0.21 | 0.44 |
| 2-6 | −0.01 | −0.14 | 3-24 | −0.03 | −0.04 | 5-22 | −0.19 | −0.19 |
| 2-7 | 0.05 | 0.0 | 3-26 | 0.0 | −0.04 | 5-23 | 0.10 | 0.13 |
| 2-8 | 0.0 | 0.07 | 3-27 | −0.05 | −0.05 | 5-24 | −0.10 | 0.06 |
| 2-9 | 0.03 | 0.04 | 3-28 | 0.02 | 0.02 | 5-25 | 0.01 | −0.03 |
| 2-11 | 0.02 | 0.02 | 3-30 | 0.03 | 0.03 | 5-26 | −0.02 | 0.0 |
| 2-12 | 0.0 | −0.01 | 3-32 | −0.02 | 0.03 | 5-32 | 0.26 | 0.44 |
| 2-13 | 0.0 | −0.01 | 3-33 | 0.0 | 0.03 | 5-33 | −0.18 | −0.17 |
| 2-14 | 0.04 | −0.02 | 3-34 | −0.08 | −0.01 | 5-34 | 0.41 | 0.40 |
| 2-15 | 0.04 | 0.05 | 3-35 | 0.0 | 0.05 | 5-36 | 0.0 | −0.22 |
| 2-16 | 0.0 | 0.01 | 3-36 | 0.0 | −0.03 | 5-42 | 0.0 | −0.04 |
| 2-19 | −0.54 | −0.51 | 3-40 | 0.0 | −0.01 | 5-43 | 0.0 | 0.08 |
| 2-20 | −0.18 | −0.15 | 3-42 | 0.0 | −0.04 | 5-44 | 0.0 | −0.04 |
| 2-21 | 0.0 | 0.04 | 3-43 | 0.0 | 0.08 | 5-45 | 0.0 | −0.05 |
| 2-22 | 0.04 | 0.04 | 3-47 | 0.0 | 0.08 | 5-47 | 0.0 | 0.04 |
| 2-23 | 0.0 | 0.08 | 3-48 | 0.0 | 0.06 | 5-48 | 0.0 | 0.19 |
| 2-24 | 0.05 | 0.05 | 3-49 | 0.0 | 0.03 | 5-49 | 0.0 | −0.17 |
| 2-26 | 0.0 | 0.03 | 3-50 | 0.0 | 0.02 | 5-50 | 0.0 | −0.10 |
| 2-27 | −0.05 | −0.05 | 4-5 | −0.01 | −0.02 | 6-7 | 0.05 | −0.01 |
| 2-28 | −0.01 | −0.01 | 4-7 | 0.02 | 0.03 | 6-8 | −0.03 | 0.04 |
| 2-30 | −0.04 | −0.04 | 4-9 | 0.0 | −0.02 | 6-10 | −0.05 | −0.05 |
| 2-32 | 0.05 | 0.07 | 4-11 | −0.02 | −0.02 | 6-15 | 0.0 | 0.01 |
| 2-33 | 0.0 | 0.03 | 4-12 | 0.02 | 0.03 | 6-16 | 0.02 | 0.02 |
| 2-34 | 0.05 | 0.02 | | | | | | |

TABLE 3 (continued)

| Term | GLY5 | GLY7 | Term | GLY5 | GLY7 | Term | GLY5 | GLY7 |
|---|---|---|---|---|---|---|---|---|
| 6-18 | 0.0 | −0.02 | 8-17 | −0.04 | −0.05 | 9-48 | 0.0 | 0.24 |
| 6-20 | 0.0 | 0.03 | 8-18 | −0.04 | −0.04 | 9-49 | 0.0 | −0.05 |
| 6-21 | 0.0 | −0.02 | 8-19 | 0.0 | 0.04 | 10-14 | 0.0 | 0.02 |
| 6-23 | −0.02 | 0.05 | 8-20 | 0.0 | 0.05 | 10-15 | 0.0 | −0.02 |
| 6-24 | −0.03 | 0.0 | 8-21 | 0.04 | −0.05 | 10-16 | 0.02 | 0.03 |
| 6-25 | −0.09 | −0.07 | 8-22 | 0.03 | 0.0 | 10-17 | 0.11 | 0.13 |
| 6-26 | 0.04 | 0.12 | 8-23 | 0.21 | 0.14 | 10-18 | 0.11 | 0.11 |
| 6-36 | 0.0 | −0.03 | 8-24 | −0.42 | −0.40 | 10-23 | 0.06 | 0.09 |
| 6-37 | −0.01 | 0.0 | 8-25 | 0.17 | 0.15 | 10-24 | 0.10 | 0.09 |
| 6-40 | −0.02 | −0.01 | 8-26 | 0.20 | 0.26 | 10-25 | 0.21 | 0.23 |
| 6-45 | 0.0 | −0.05 | 8-32 | −0.02 | −0.03 | 10-26 | −0.18 | −0.19 |
| 6-49 | 0.0 | −0.04 | 8-33 | 0.0 | −0.02 | 10-32 | 0.04 | −0.01 |
| 6-50 | 0.0 | −0.03 | 8-34 | −0.05 | −0.05 | 10-36 | 0.0 | 0.02 |
| 7-8 | 1.28 | 1.24 | 8-35 | 0.0 | −0.04 | 10-37 | −0.51 | −0.50 |
| 7-9 | 0.42 | 0.39 | 8-36 | 0.0 | 0.07 | 10-38 | 0.0 | −0.01 |
| 7-10 | −0.08 | −0.05 | 8-37 | 0.04 | 0.05 | 10-40 | −0.05 | −0.04 |
| 7-11 | 0.0 | −0.01 | 8-38 | −0.02 | −0.03 | 10-45 | 0.0 | −0.03 |
| 7-14 | −0.02 | 0.03 | 8-40 | 0.07 | 0.07 | 10-48 | 0.0 | −0.01 |
| 7-15 | −0.02 | −0.02 | 8-42 | 0.0 | 0.06 | 11-12 | 0.01 | 0.02 |
| 7-16 | −0.02 | −0.03 | 8-43 | 0.0 | −0.02 | 11-13 | 0.01 | 0.01 |
| 7-17 | 0.04 | 0.05 | 8-45 | 0.0 | −0.06 | 11-19 | 0.06 | 0.06 |
| 7-18 | 0.04 | 0.04 | 8-47 | 0.0 | −0.10 | 11-20 | −0.05 | −0.05 |
| 7-20 | −0.03 | −0.03 | 8-48 | 0.0 | −0.13 | 11-27 | 0.05 | 0.05 |
| 7-21 | 0.02 | 0.04 | 8-49 | 0.0 | −0.02 | 11-28 | −0.10 | −0.10 |
| 7-22 | −0.05 | −0.01 | 8-50 | 0.0 | −0.02 | 11-30 | 0.10 | 0.10 |
| 7-23 | −0.56 | −0.42 | 9-10 | −0.02 | −0.03 | 11-32 | 0.01 | 0.0 |
| 7-24 | −0.05 | −0.11 | 9-11 | 0.01 | 0.02 | 12-13 | 0.03 | 0.03 |
| 7-25 | −0.04 | −0.04 | 9-14 | 0.02 | −0.02 | 12-14 | −0.01 | 0.0 |
| 7-26 | 0.04 | 0.05 | 9-15 | 0.02 | 0.03 | 12-15 | 0.0 | −0.01 |
| 7-32 | 0.04 | 0.08 | 9-16 | 0.02 | 0.02 | 12-19 | −0.04 | −0.03 |
| 7-33 | −0.02 | 0.0 | 9-19 | 0.0 | −0.01 | 12-20 | 0.03 | 0.03 |
| 7-34 | −0.04 | −0.04 | 9-20 | −0.02 | −0.08 | 12-27 | 0.06 | 0.05 |
| 7-35 | 0.0 | 0.05 | 9-21 | 0.01 | 0.19 | 12-28 | 0.06 | 0.06 |
| 7-36 | 0.0 | −0.06 | 9-22 | 0.04 | 0.0 | 12-29 | 0.09 | 0.10 |
| 7-37 | −0.02 | −0.04 | 9-23 | 0.10 | 0.41 | 12-30 | −0.05 | −0.05 |
| 7-38 | 0.02 | 0.02 | 9-24 | 0.42 | 0.21 | 12-31 | 0.10 | 0.10 |
| 7-40 | −0.03 | −0.04 | 9-25 | 0.03 | 0.0 | 12-42 | 0.02 | 0.02 |
| 7-42 | 0.0 | −0.02 | 9-26 | 0.02 | 0.04 | 12-47 | 0.01 | 0.0 |
| 7-43 | 0.0 | 0.02 | 9-32 | 0.54 | 0.26 | 12-48 | 0.0 | −0.01 |
| 7-44 | 0.0 | 0.02 | 9-33 | −0.12 | −0.12 | 13-15 | −0.01 | 0.0 |
| 7-47 | 0.0 | 0.05 | 9-34 | −0.22 | −0.23 | 13-19 | −0.04 | −0.04 |
| 7-48 | 0.0 | 0.05 | 9-35 | 0.0 | 0.02 | 13-20 | 0.03 | 0.03 |
| 7-49 | 0.0 | 0.01 | 9-36 | 0.0 | −0.17 | 13-21 | 0.0 | −0.01 |
| 8-9 | 0.27 | 0.23 | 9-37 | 0.0 | −0.01 | 13-27 | 0.06 | 0.05 |
| 8-10 | 0.10 | 0.11 | 9-42 | 0.0 | −0.06 | 13-28 | 0.06 | 0.05 |
| 8-14 | 0.01 | 0.0 | 9-43 | 0.0 | 0.10 | 13-29 | −0.09 | −0.09 |
| 8-15 | 0.01 | 0.01 | 9-44 | 0.0 | 0.05 | 13-30 | −0.05 | −0.05 |
| 8-16 | −0.02 | −0.02 | 9-47 | 0.0 | 0.11 | 13-31 | −0.10 | −0.09 |

TABLE 3 (continued)

| Term | GLY5 | GLY7 | Term | GLY5 | GLY7 | Term | GLY5 | GLY7 |
|---|---|---|---|---|---|---|---|---|
| 13-32 | 0.0 | −0.02 | 17-38 | 0.06 | 0.07 | 20-33 | 0.02 | −0.01 |
| 13-42 | −0.02 | −0.02 | 17-39 | 0.10 | 0.10 | 20-34 | 0.02 | 0.0 |
| 13-46 | 0.0 | 0.01 | 17-40 | −0.03 | −0.03 | 20-35 | 0.0 | −0.01 |
| 13-47 | −0.01 | 0.0 | 17-41 | 0.05 | 0.05 | 20-36 | 0.0 | 0.14 |
| 14-15 | 0.07 | 0.01 | 17-45 | −0.01 | −0.02 | 20-42 | 0.0 | 0.05 |
| 14-17 | −0.01 | 0.0 | 17-47 | 0.01 | 0.0 | 20-43 | 0.0 | −0.06 |
| 14-19 | 0.01 | 0.0 | 17-49 | 0.01 | 0.0 | 20-44 | 0.0 | −0.02 |
| 14-21 | −0.04 | 0.0 | 17-51 | 0.03 | 0.02 | 20-45 | 0.0 | 0.01 |
| 14-22 | 0.0 | 0.01 | 18-23 | 0.01 | 0.02 | 20-47 | 0.0 | −0.06 |
| 14-23 | −0.02 | 0.06 | 18-25 | −0.03 | −0.04 | 20-48 | 0.0 | −0.14 |
| 14-24 | 0.01 | −0.05 | 18-37 | 0.06 | 0.06 | 20-49 | 0.0 | 0.04 |
| 14-32 | −0.06 | −0.06 | 18-38 | 0.06 | 0.06 | 21-22 | 0.02 | −0.01 |
| 14-33 | 0.07 | 0.06 | 18-39 | −0.10 | −0.10 | 21-23 | 0.03 | 0.22 |
| 14-34 | 0.0 | −0.01 | 18-40 | −0.03 | −0.03 | 21-25 | 0.0 | −0.04 |
| 14-35 | −0.02 | −0.02 | 18-41 | −0.05 | −0.06 | 21-26 | 0.0 | −0.02 |
| 14-36 | 0.09 | 0.11 | 18-45 | 0.01 | 0.02 | 21-30 | 0.04 | 0.04 |
| 14-44 | 0.02 | 0.0 | 18-47 | −0.01 | 0.0 | 21-32 | 0.0 | 0.28 |
| 14-48 | 0.04 | −0.02 | 18-49 | −0.01 | 0.0 | 21-34 | −0.03 | 0.01 |
| 14-49 | −0.01 | 0.0 | 18-51 | −0.03 | −0.02 | 21-35 | 0.0 | 0.04 |
| 14-50 | 0.01 | 0.0 | 19-20 | 0.14 | 0.19 | 21-36 | 0.0 | −0.27 |
| 15-17 | 0.0 | −0.01 | 19-21 | 0.09 | 0.0 | 21-40 | 0.01 | 0.0 |
| 15-18 | −0.01 | 0.0 | 19-22 | −0.02 | −0.02 | 21-42 | 0.0 | −0.06 |
| 15-19 | 0.01 | 0.02 | 19-23 | 0.02 | −0.03 | 21-43 | 0.0 | 0.12 |
| 15-20 | 0.0 | 0.02 | 19-24 | −0.02 | 0.01 | 21-44 | 0.0 | 0.06 |
| 15-21 | −0.04 | −0.05 | 19-26 | 0.0 | 0.03 | 21-45 | 0.0 | −0.07 |
| 15-23 | −0.02 | −0.05 | 19-27 | −0.03 | −0.03 | 21-47 | 0.0 | 0.08 |
| 15-24 | 0.01 | 0.03 | 19-28 | 0.04 | 0.04 | 21-48 | 0.0 | 0.24 |
| 15-32 | −0.06 | −0.04 | 19-30 | 0.12 | 0.12 | 21-49 | 0.0 | −0.23 |
| 15-33 | 0.07 | 0.05 | 19-32 | 0.01 | −0.04 | 21-50 | 0.0 | −0.10 |
| 15-35 | 0.02 | 0.02 | 19-33 | 0.0 | −0.02 | 21-51 | 0.0 | −0.01 |
| 15-36 | −0.09 | −0.11 | 19-34 | 0.01 | 0.01 | 22-23 | −0.03 | 0.0 |
| 15-44 | −0.02 | 0.01 | 19-36 | 0.0 | 0.07 | 22-24 | 0.04 | 0.0 |
| 15-48 | −0.04 | 0.04 | 19-42 | 0.0 | 0.02 | 22-32 | 0.06 | 0.0 |
| 15-49 | 0.01 | −0.01 | 19-43 | 0.0 | −0.03 | 22-33 | 0.02 | 0.0 |
| 15-50 | −0.01 | 0.0 | 19-47 | 0.0 | −0.02 | 22-34 | −0.04 | −0.02 |
| 16-17 | 0.02 | 0.02 | 19-48 | 0.0 | −0.05 | 22-35 | 0.0 | 0.03 |
| 16-18 | 0.02 | 0.02 | 19-49 | 0.0 | 0.02 | 22-36 | 0.0 | 0.03 |
| 16-25 | 0.02 | 0.03 | 20-21 | 0.03 | −0.15 | 23-24 | 0.03 | 0.08 |
| 16-26 | 0.01 | 0.0 | 20-22 | −0.04 | −0.05 | 23-25 | 0.05 | 0.0 |
| 16-37 | 0.06 | 0.06 | 20-23 | 0.02 | −0.09 | 23-26 | −0.02 | 0.04 |
| 16-38 | −0.12 | −0.12 | 20-24 | −0.04 | 0.0 | 23-32 | 0.06 | 0.19 |
| 16-40 | 0.08 | 0.08 | 20-26 | 0.0 | 0.03 | 23-33 | 0.04 | −0.04 |
| 17-18 | 0.05 | 0.05 | 20-27 | −0.02 | −0.02 | 23-34 | 0.02 | −0.05 |
| 17-23 | 0.01 | 0.02 | 20-28 | −0.02 | −0.02 | 23-35 | 0.0 | −0.06 |
| 17-25 | −0.03 | −0.03 | 20-30 | −0.09 | −0.08 | 23-36 | 0.0 | −0.12 |
| 17-37 | 0.06 | 0.06 | 20-32 | 0.0 | −0.11 | 23-37 | −0.02 | −0.02 |

TABLE 3 (continued)

| Term | GLY5 | GLY7 | Term | GLY5 | GLY7 | Term | GLY5 | GLY7 |
|---|---|---|---|---|---|---|---|---|
| 23-40 | 0.04 | 0.02 | 30-36 | 0.0 | −0.01 | 39-45 | −0.02 | −0.02 |
| 23-42 | 0.0 | −0.08 | 30-49 | 0.0 | −0.01 | 41-44 | −0.02 | −0.02 |
| 23-43 | 0.0 | 0.12 | 31-42 | 0.09 | 0.10 | 41-45 | −0.03 | −0.02 |
| 23-44 | 0.0 | 0.04 | 31-46 | 0.03 | 0.04 | 41-50 | 0.0 | −0.01 |
| 23-47 | 0.0 | 0.10 | 31-47 | 0.02 | 0.02 | 41-51 | 0.05 | 0.05 |
| 23-48 | 0.0 | 0.26 | 32-33 | 0.0 | 0.01 | 42-43 | −0.03 | −0.09 |
| 23-49 | 0.0 | −0.07 | 32-34 | −0.03 | −0.06 | 42-44 | −0.02 | 0.0 |
| 24-25 | 0.05 | 0.05 | 32-35 | 0.0 | 0.03 | 42-45 | 0.0 | −0.03 |
| 24-26 | −0.06 | −0.06 | 32-36 | 0.0 | −0.29 | 42-46 | −0.04 | −0.05 |
| 24-32 | 0.14 | 0.02 | 32-40 | −0.01 | 0.0 | 42-47 | −0.06 | −0.14 |
| 24-33 | −0.03 | 0.0 | 32-42 | 0.0 | −0.05 | 42-48 | −0.06 | −0.18 |
| 24-34 | −0.04 | 0.0 | 32-43 | 0.0 | 0.19 | 42-49 | −0.02 | −0.06 |
| 24-35 | 0.0 | 0.06 | 32-45 | 0.0 | −0.02 | 42-50 | −0.01 | −0.03 |
| 24-36 | 0.0 | −0.02 | 32-47 | 0.0 | 0.06 | 43-44 | 0.0 | 0.04 |
| 24-37 | −0.02 | −0.01 | 32-48 | 0.0 | 0.28 | 43-45 | −0.02 | 0.0 |
| 24-38 | 0.02 | 0.02 | 32-49 | 0.0 | −0.16 | 43-46 | 0.02 | 0.02 |
| 24-40 | 0.01 | 0.01 | 33-34 | −0.02 | −0.02 | 43-47 | −0.11 | −0.02 |
| 24-42 | 0.0 | 0.02 | 33-35 | 0.0 | −0.02 | 43-48 | −0.02 | 0.17 |
| 24-43 | 0.0 | −0.02 | 33-44 | 0.0 | −0.02 | 43-49 | −0.09 | −0.02 |
| 24-47 | 0.0 | −0.03 | 33-48 | 0.0 | −0.01 | 43-50 | 0.0 | 0.03 |
| 24-48 | 0.0 | −0.05 | 33-50 | 0.0 | −0.01 | 44-45 | −0.04 | −0.06 |
| 24-49 | 0.0 | 0.02 | 34-42 | 0.0 | −0.01 | 44-46 | 0.02 | 0.0 |
| 25-26 | −0.02 | −0.07 | 34-43 | 0.0 | −0.02 | 44-47 | 0.02 | −0.06 |
| 25-32 | 0.05 | −0.06 | 34-44 | 0.0 | −0.03 | 44-48 | 0.11 | 0.01 |
| 25-35 | 0.0 | −0.02 | 34-48 | 0.0 | 0.01 | 44-49 | 0.0 | −0.09 |
| 25-36 | 0.0 | 0.07 | 34-49 | 0.0 | −0.02 | 44-50 | −0.02 | −0.02 |
| 25-40 | 0.03 | 0.04 | 35-36 | 0.08 | 0.04 | 45-47 | 0.01 | 0.07 |
| 25-42 | 0.0 | 0.02 | 35-42 | −0.04 | −0.05 | 45-48 | −0.01 | 0.06 |
| 25-43 | 0.0 | −0.03 | 35-43 | −0.03 | 0.03 | 45-49 | 0.03 | 0.13 |
| 25-44 | 0.0 | −0.01 | 35-44 | −0.04 | 0.0 | 45-50 | −0.06 | 0.0 |
| 25-47 | 0.0 | −0.02 | 35-45 | 0.0 | 0.04 | 45-51 | 0.02 | 0.02 |
| 25-48 | 0.0 | −0.06 | 35-47 | 0.03 | 0.07 | 46-48 | 0.03 | 0.02 |
| 25-49 | 0.0 | 0.02 | 35-48 | 0.13 | 0.09 | 47-48 | 0.09 | 0.28 |
| 25-50 | 0.0 | 0.02 | 35-49 | 0.06 | 0.09 | 47-49 | 0.10 | 0.08 |
| 26-32 | −0.02 | 0.03 | 35-50 | 0.0 | 0.06 | 47-50 | 0.04 | 0.03 |
| 26-34 | −0.01 | 0.0 | 36-42 | 0.0 | 0.07 | 47-51 | 0.02 | 0.0 |
| 26-36 | 0.0 | −0.02 | 36-43 | −0.05 | −0.11 | 48-49 | 0.12 | 0.05 |
| 26-37 | 0.03 | 0.02 | 36-44 | 0.02 | −0.06 | 48-50 | 0.06 | 0.06 |
| 26-40 | 0.03 | 0.03 | 36-45 | 0.01 | 0.03 | 48-51 | 0.01 | 0.0 |
| 26-47 | 0.0 | −0.02 | 36-47 | 0.0 | −0.12 | 49-50 | 0.0 | 0.17 |
| 26-49 | 0.0 | −0.01 | 36-48 | −0.02 | −0.32 | 49-51 | 0.02 | 0.02 |
| 28-30 | −0.01 | −0.01 | 36-49 | 0.08 | 0.13 | 50-51 | 0.02 | 0.03 |
| 29-31 | 0.0 | −0.01 | 36-50 | −0.01 | 0.06 | | | |
| 29-42 | −0.01 | −0.01 | 38-40 | −0.03 | −0.03 | | | |
| 29-46 | 0.02 | 0.02 | 39-41 | 0.03 | 0.03 | | | |
| 29-47 | −0.02 | −0.02 | 39-44 | 0.02 | 0.01 | | | |

[a]Units: energy in mdyn Å, stretching coordinates in Å, bending coordinates in radians.

TABLE 4

Scaled diagonal and off-diagonal force constants, $|F_{ij}| \geq 0.1$, compared with empirical force fields[a]

| | GLY5 | GLY7 | PGI | Gly-Gly | Alkane |
|---|---|---|---|---|---|
| NH str1 | 6.397 | 6.523 | 5.840 | 5.964 | |
| CO str1 | 11.167 | 10.720 | 9.882 | 8.9 | |
| CN str1 | 6.607 | 6.636 | 6.415 | 6.9 | |
| MC str | 4.186 | 4.200 | | | 4.450 |
| $NC^{\alpha}$ str | 5.356 | 5.081 | 5.043 | 4.6 | 4.453 |
| NH str2 | 6.511 | 6.246 | 5.840 | 5.964 | |
| CO str2 | 10.983 | 11.262 | 9.882 | 8.9 | |
| CN str2 | 6.773 | 6.937 | 6.415 | 6.9 | |
| $C^{\alpha}C$ str | 4.293 | 4.055 | 4.409 | | 4.453 |
| NM str | 5.204 | 5.290 | | | 4.450 |
| MH1 str | 4.973 | 4.986 | | | |
| MH2 str | 4.798 | 4.792 | | | |
| MH3 str | 4.798 | 4.810 | | | |
| CH10 str | 4.737 | 4.995 | 4.564 | | 4.538 |
| CH11 str | 4.737 | 4.909 | 4.564 | | 4.538 |
| MH19 str | 4.872 | 4.862 | | | |
| MH17 str | 4.820 | 4.751 | | | |
| MH18 str | 4.820 | 4.803 | | | |
| MCN def | 0.952 | 0.996 | | | |
| CO ib1 | 1.111 | 1.201 | 1.246 | 1.17 | |
| $CNC^{\alpha}$ def | 0.812 | 1.154 | 0.662 | 1.3 | |
| NH ib1 | 0.549 | 0.585 | 0.521 | 0.525 | |
| $C^{\alpha}CN$ def | 0.955 | 1.156 | 1.349 | 1.4 | |
| CO ib2 | 1.222 | 1.063 | 1.246 | 1.17 | |
| CNM def | 0.783 | 0.813 | | | |
| NH ib2 | 0.588 | 0.642 | 0.521 | 0.525 | |
| M1 sb | 0.545 | 0.547 | | | 0.585 |
| M1 ab1 | 0.521 | 0.519 | | | 0.535 |
| M1 ab2 | 0.522 | 0.521 | | | 0.535 |
| M1 rock1 | 0.647 | 0.653 | | | 0.705 |
| M1 rock2 | 0.579 | 0.582 | | | 0.705 |
| $NC^{\alpha}C$ def | 1.432 | 1.220 | 0.833 | 1.0 | 0.941 |
| $CH_2$ bend | 0.558 | 0.543 | 0.531 | 0.549 | 0.589 |
| $CH_2$ wag | 0.645 | 0.655 | 0.688 | 0.7 | 0.622 |
| $CH_2$ twist | 0.669 | 0.701 | 0.673 | 0.696 | 0.639 |
| $CH_2$ rock | 0.731 | 0.992 | 0.711 | 0.68 | 0.766 |
| M2 sb | 0.607 | 0.606 | | | 0.585 |
| M2 ab1 | 0.544 | 0.548 | | | 0.535 |
| M2 ab2 | 0.535 | 0.541 | | | 0.535 |
| M2 rock1 | 0.785 | 0.780 | | | 0.705 |
| M2 rock2 | 0.771 | 0.765 | | | 0.705 |
| CO ob1 | 0.766 | 0.802 | 0.587 | 0.75 | |
| NH ob1 | 0.205 | 0.250 | 0.129 | 0.273 | |
| CO ob2 | 0.789 | 0.780 | 0.587 | 0.75 | |
| NH ob2 | 0.165 | 0.219 | 0.129 | 0.273 | |
| MC tor | 0.061 | 0.059 | | | 0.086 |
| CN tor1 | 0.447 | 0.541 | 0.680 | 0.128 | |
| $NC^{\alpha}$ tor | 0.250 | 0.530 | 0.037 | 0.036 | 0.107 |
| $C^{\alpha}C$ tor | 0.267 | 0.315 | 0.037 | 0.036 | 0.107 |
| CN tor2 | 0.367 | 0.506 | 0.680 | 0.128 | |

TABLE 4 (continued)

| | GLY5 | GLY7 | PGI | Gly-Gly | Alkane |
|---|---|---|---|---|---|
| NM tor | 0.050 | 0.053 | | | 0.086 |
| NH str1-$NC^{\alpha}$ str | 0.116 | 0.0 | 0.0 | | |
| NH str1-$CNC^{\alpha}$ def | −0.112 | −0.091 | 0.0 | | |
| NH str1-NH ib1 | −0.106 | 0.024 | 0.0 | | |
| CO str1-CN str1 | 1.350 | 1.352 | 0.500 | 0.6 | |
| CO str1-MC str | 0.360 | 0.349 | | | |
| CO str1-NH str2 | −0.013 | −0.143 | 0.0 | | |
| CO str1-MCN def | −0.536 | −0.510 | | | |
| CO str1-CO ib1 | −0.177 | −0.146 | 0.0 | | |
| CN str1-MC str | 0.297 | 0.298 | | | |
| CN str1-$NC^{\alpha}$ str | 0.150 | 0.235 | 0.300 | | |
| CN str1-MCN def | 0.173 | 0.155 | | | |
| CN str1-CO ib1 | −0.422 | −0.490 | −0.141 | −0.45 | |
| CN str1-$CNC^{\alpha}$ def | 0.176 | 0.214 | 0.125 | | |
| CN str1-NH ib1 | 0.165 | 0.197 | 0.208 | 0.0 | |
| MC str-MCN def | 0.201 | 0.210 | | | |
| MC str-CO ib1 | 0.241 | 0.247 | | | |
| MC str-M1 sb | −0.289 | −0.298 | | | −0.436 |
| $NC^{\alpha}$ str-$C^{\alpha}C$ str | 0.124 | 0.309 | 0.300 | | 0.199 |
| $NC^{\alpha}$str-CH10 str | 0.128 | 0.046 | 0.0 | | |
| $NC^{\alpha}$ str-CH11 str | 0.128 | 0.086 | 0.0 | | |
| $NC^{\alpha}$ str-$CNC^{\alpha}$ def | 0.213 | 0.435 | 0.125 | | |
| $NC^{\alpha}$ str-NH ib1 | −0.193 | −0.187 | −0.208 | −0.258 | |
| $NC^{\alpha}$ str-$C^{\alpha}CN$ def | 0.100 | 0.125 | 0.0 | | |
| $NC^{\alpha}$ str-$NC^{\alpha}C$ def | 0.262 | 0.440 | 0.076 | 0.35 | 0.213 |
| $NC^{\alpha}$ str-$CH_2$ bend | −0.181 | −0.170 | −0.243 | | 0.0 |
| $NC^{\alpha}$ str-$CH_2$ wag | 0.410 | 0.402 | 0.491 | | 0.314 |
| $NC^{\alpha}$ str-$CH_2$ rock | 0.0 | −0.220 | 0.0 | | 0.0 |
| $NC^{\alpha}$ str-$NC^{\alpha}$ tor | 0.0 | 0.193 | 0.0 | | |
| $NC^{\alpha}$ str-$C^{\alpha}C$ tor | 0.0 | −0.166 | 0.0 | | |
| NH str2-NH ib2 | 0.041 | 0.115 | 0.0 | | |
| CO str2-CN str2 | 1.284 | 1.243 | 0.500 | 0.6 | |
| CO str2-$C^{\alpha}C$ str | 0.420 | 0.386 | 0.500 | | |
| CO str2-$C^{\alpha}CN$ def | −0.556 | −0.424 | −0.490 | −0.5 | |
| CO str2-CO ib2 | −0.050 | −0.108 | 0.0 | | |
| CN str2-$C^{\alpha}C$ str | 0.267 | 0.233 | 0.300 | | |
| CN str2-NM str | 0.096 | 0.111 | | | |
| CN str2-$C^{\alpha}CN$ def | 0.212 | 0.136 | 0.163 | | |
| CN str2-CO ib2 | −0.423 | −0.399 | −0.141 | −0.45 | |
| CN str2-CNM def | 0.165 | 0.149 | | | |
| CN str2-NH ib2 | 0.197 | 0.259 | 0.208 | 0.0 | |
| CN str2-$NC^{\alpha}$ tor | 0.0 | −0.127 | 0.0 | | |
| $C^{\alpha}C$ str-$CNC^{\alpha}$ def | 0.013 | 0.188 | 0.0 | | |
| $C^{\alpha}C$ str-$C^{\alpha}CN$ def | 0.101 | 0.410 | 0.163 | | |
| $C^{\alpha}C$ str-CO ib2 | 0.416 | 0.206 | 0.141 | 0.4 | |
| $C^{\alpha}C$ str-$NC^{\alpha}C$ def | 0.538 | 0.259 | 0.190 | | 0.213 |
| $C^{\alpha}C$ str-$CH_2$ bend | −0.117 | −0.119 | −0.103 | −0.162 | 0.0 |
| $C^{\alpha}C$ str-$CH_2$ wag | −0.218 | −0.232 | −0.179 | −0.158 | −0.314 |
| $C^{\alpha}C$ str-$CH_2$ rock | 0.0 | −0.171 | 0.0 | | 0.0 |
| $C^{\alpha}C$ str-NH ob1 | 0.0 | 0.101 | 0.0 | | |

TABLE 4 (continued)

| | GLY5 | GLY7 | PGI | Gly-Gly | Alkane |
|---|---|---|---|---|---|
| $C^{\alpha}C$ str-CN tor1 | 0.0 | 0.111 | 0.0 | | |
| $C^{\alpha}C$ str-$NC^{\alpha}$ tor | 0.0 | 0.240 | 0.0 | | |
| NM str-MH17 str | 0.105 | 0.127 | | | |
| NM str-MH18 str | 0.105 | 0.107 | | | |
| NM str-CNM def | 0.206 | 0.232 | | | |
| NM str-NH ib2 | −0.183 | −0.185 | | | |
| NM str-M2 sb | −0.507 | −0.502 | | | −0.436 |
| CH10 str-$CH_2$ rock | 0.093 | 0.107 | 0.0 | | |
| CH11 str-$CH_2$ rock | −0.093 | −0.111 | 0.0 | | |
| MH19 str-M2 ab1 | −0.115 | −0.116 | | | |
| MH17 str-M2 ab2 | 0.096 | 0.100 | | | |
| MCN def-CO ib1 | 0.145 | 0.190 | | | |
| MCN def-M1 rock1 | 0.123 | 0.118 | | | |
| CO ib1-$CNC^{\alpha}$ def | 0.027 | −0.147 | 0.072 | | |
| CO ib1-$NC^{\alpha}C$ def | 0.0 | −0.113 | 0.0 | | |
| CO ib1-$CH_2$ rock | 0.0 | 0.138 | −0.018 | | |
| CO ib1-$NC^{\alpha}$ tor | 0.0 | −0.138 | 0.0 | | |
| $CNC^{\alpha}$ def-$C^{\alpha}CN$ def | 0.028 | 0.222 | 0.0 | | |
| $CNC^{\alpha}$ def-$NC^{\alpha}C$ def | 0.0 | 0.278 | 0.047 | | |
| $CNC^{\alpha}$ def-$CH_2$ rock | 0.0 | −0.271 | 0.014 | | |
| $CNC^{\alpha}$ def-NH ob1 | 0.0 | 0.120 | 0.0 | | |
| $CNC^{\alpha}$ def-$NC^{\alpha}$ tor | 0.0 | 0.237 | 0.0 | | |
| $CNC^{\alpha}$ def-$C^{\alpha}C$ tor | 0.0 | −0.228 | 0.0 | | |
| $C^{\alpha}CN$ def-$NC^{\alpha}C$ def | 0.059 | 0.187 | 0.019 | | |
| $C^{\alpha}CN$ def-$CH_2$ rock | 0.0 | −0.122 | 0.010 | | |
| $C^{\alpha}CN$ def-NH ob1 | 0.0 | 0.118 | 0.0 | | |
| $C^{\alpha}CN$ def-CN tor1 | 0.0 | 0.103 | 0.0 | | |
| $C^{\alpha}CN$ def-$NC^{\alpha}$ tor | 0.0 | 0.260 | 0.0 | | |
| CO ib2-$NC^{\alpha}C$ def | 0.141 | 0.016 | −0.032 | | |
| $NC^{\alpha}C$ def-$CH_2$ rock | 0.0 | −0.292 | 0.0 | | |
| $NC^{\alpha}C$ def-NH ob1 | 0.0 | 0.189 | 0.073 | | |
| $NC^{\alpha}C$ def-$NC^{\alpha}$ tor | 0.0 | 0.281 | 0.0 | | |
| $NC^{\alpha}C$ def-$C^{\alpha}C$ tor | 0.0 | −0.159 | 0.0 | | |
| $CH_2$ twist-$NC^{\alpha}$ tor | 0.132 | 0.090 | 0.0 | | |
| $CH_2$ rock-NH ob1 | −0.048 | −0.112 | −0.028 | | |
| $CH_2$ rock-CN tor1 | 0.0 | −0.118 | 0.0 | | |
| $Ch_2$ rock-$NC^{\alpha}$ tor | −0.016 | −0.317 | 0.0 | | |
| $CH_2$ rock-$C^{\alpha}C$ tor | 0.082 | 0.125 | 0.0 | | |
| CO ob1-CN tor1 | −0.065 | −0.141 | 0.011 | | |
| CO ob1-$NC^{\alpha}$ tor | −0.057 | −0.177 | 0.0 | | |
| NH ob1-CN tor1 | −0.113 | −0.015 | −0.168 | | |
| NH ob1-$NC^{\alpha}$ tor | −0.025 | 0.167 | 0.0 | | |
| CO ob2-$NC^{\alpha}$ tor | 0.109 | 0.012 | 0.0 | | |
| NH ob2-$C^{\alpha}C$ tor | 0.032 | 0.129 | 0.0 | | |
| CN tor1-$NC^{\alpha}$ tor | 0.087 | 0.281 | 0.0 | | |
| CN tor1-$C^{\alpha}C$ tor | 0.104 | 0.084 | 0.0 | | |
| $NC^{\alpha}$ tor-$C^{\alpha}C$ tor | 0.122 | 0.050 | 0.0 | | |
| $C^{\alpha}C$ tor-CN tor2 | 0.0 | 0.169 | 0.0 | | |

[a]Units: energy in mdyn-Å, stretching coordinates in Å, bending coordinates in radians. PGI: ref. 46, Gly-Gly: ref. 47, alkane: ref. 48.

TABLE 5

Diagonal cubic force constants[a]

| | GLY5 | GLY7 | | GLY5 | GLY7 |
|---|---|---|---|---|---|
| NH str1 | −51.30 | −56.39 | NH ib2 | −0.04 | 0.61 |
| CO str1 | −79.63 | −87.94 | M1 sb | −0.14 | −0.12 |
| CN str1 | −40.65 | −46.28 | M1 ab1 | −0.26 | −0.25 |
| MC str | −19.40 | −22.09 | M1 ab2 | 0.00 | −0.01 |
| $NC^{\alpha}$ str | −24.62 | −24.32 | M1 rock1 | −0.48 | −0.43 |
| NH str2 | −53.54 | −55.89 | M1 rock2 | 0.00 | 0.01 |
| CO str2 | −98.96 | −131.65 | $NC^{\alpha}C$ def | −4.56 | −3.05 |
| CN str2 | −51.59 | −55.29 | $CH_2$ bend | −0.24 | −0.13 |
| $C^{\alpha}C$ str | −32.11 | −19.81 | $CH_2$ wag | 0.03 | −0.12 |
| NM str | −26.59 | −33.89 | $CH_2$ twist | 0.00 | 0.02 |
| MH1 str | −36.02 | −33.51 | $CH_2$ rock | 0.00 | 0.89 |
| MH2 str | −34.62 | −33.17 | M2 sb | −0.05 | 0.12 |
| MH3 str | −34.62 | −33.19 | M2 ab1 | −0.20 | −0.20 |
| CH10 str | −37.62 | −35.10 | M2 ab2 | 0.00 | 0.01 |
| CH11 str | −37.59 | −35.85 | M2 rock1 | −0.41 | −0.49 |
| MH19 str | −36.11 | −35.15 | M2 rock2 | 0.00 | 0.01 |
| MH17 str | −35.15 | −33.97 | CO ob1 | 0.00 | −0.07 |
| MH18 str | −35.15 | −33.67 | NH ob1 | 0.00 | −0.38 |
| MCN def | −2.60 | −2.35 | CO ob2 | 0.00 | −0.05 |
| CO ib1 | 0.05 | 0.42 | NH ob2 | 0.00 | −0.05 |
| $CNC^{\alpha}$ def | −1.83 | −4.29 | MC tor | 0.00 | 0.00 |
| NH ib1 | −0.13 | 0.02 | CN tor1 | 0.00 | −0.70 |
| $C^{\alpha}CN$ def | −0.90 | −1.43 | $NC^{\alpha}$ tor | 0.00 | −4.08 |
| CO ib2 | −0.53 | 0.07 | $C^{\alpha}C$ tor | 0.00 | 0.52 |
| CNM def | −0.83 | −1.43 | CN tor2 | 0.00 | −0.13 |
| | | | NM tor | 0.00 | 0.04 |

[a]Units: stretches, mdyn $Å^{-2}$; bends and torsions, mdyn-Å $rad^{-3}$.

GLY7 differ by no more than 6 $cm^{-1}$ from those obtained with all scaled $|F_{ij}| \geq 0.001$. We will discuss the force fields and frequencies separately. Except for highly localized modes such as the NH stretches, frequencies may not be as readily correlated with structure as may force constants because each normal mode depends on several internal coordinate force constants which may vary in competing or uncorrelated ways. Also, frequencies depend on structure both through structure-dependent force constants and through the **B** matrix.

As noted earlier, the force fields of GLY5 and GLY7 are expected to reflect the changes in conformation and hydrogen bonding. We consider first the effects of the $C_5$ and $C_7$ hydrogen bonds on the force constants of the CONH groups. From Table 4, we see that the changes in the NH and CO stretch (str) force constants are clearly due primarily to the hydrogen bonds. Thus, in GLY5 $f$(NH str1) is less than $f$(NH str2) whereas $f$(CO str1) is greater than $f$(CO str2), the $C_5$ hydrogen bond being formed between the $N_7H_8$ and $C_{12}O_{13}$ bonds.

TABLE 6

Normal modes of GLY5 and GLY7 using scaled force constants

| $\nu$ ($cm^{-1}$) | $I^a$ | Potential energy distribution > 10% |
|---|---|---|
| | | *GLY5* |
| 3431 | 23 | NH str2(99) |
| 3400 | 71 | NH str1(99) |
| 3023 | 3 | MH1 str(84) |
| 3000 | 6 | MH19 str(71),MH17 str(15),MH18 str(15) |
| 2980 | 13 | MH17str(50),MH18 str(50) |
| 2972 | 3 | MH2 str(50),MH3 str(50) |
| 2944 | 2 | CH10 str(49),CH11 str(49) |
| 2920 | 3 | CH10 str(44),CH11 str(44) |
| 2907 | 39 | MH17 str(30),MH18 str(30),MH19 str(25) |
| 2904 | 1 | MH2 str(35),MH3 str(35),MH1 str(14) |
| 1706 | 24 | CO str1(50),CO str2(33) |
| 1678 | 444 | CO str2(47),CO str1(37) |
| 1556 | 206 | NH ib2(53),CN str2(29) |
| 1521 | 635 | NH ib1(55),CN str1(28) |
| 1476 | 2 | M2 ab1(92) |
| 1459 | 20 | $CH_2$ bend(98) |
| 1453 | 7 | M2 ab2(95) |
| 1444 | 9 | M1 ab2(94) |
| 1436 | 33 | M1 ab1(91) |
| 1413 | 1 | M2 sb(102) |
| 1370 | 70 | M1 sb(74),MC str(12),$CH_2$ wag(10) |
| 1352 | 121 | $CH_2$ wag(34),M1 sb(27),$C^{\alpha}C$ str(15) |
| 1279 | 1 | CN str1(21),NH ib1(19),CN str2(15),CO ib1(10) |
| 1242 | 106 | $CH_2$ wag(44),CN str2(17),NM str(10) |
| 1205 | 1 | $CH_2$ twist(97) |
| 1172 | 2 | M2 rock1(50),$NC^{\alpha}$ str(11) |
| 1148 | 1 | $NC^{\alpha}$ str(52),M2 rock1(15) |
| 1119 | 1 | M2 rock2(91) |
| 1055 | 22 | M1 rock2(68),CO ob1(17) |
| 1043 | 15 | NM str(56),$C^{\alpha}C$ str(13),M1 rock1(11) |
| 990 | 9 | $CH_2$ rock(75),CO ob2(21) |
| 983 | 20 | M1 rock1(52),$NC^{\alpha}$ str(12),CN str1(10) |
| 974 | 14 | MC str(24),$CNC^{\alpha}$ def(14) |
| 874 | 3 | $C^{\alpha}C$ str(25),CN str2(15),M2 rock1(13) |
| 699 | 11 | CO ib2(33),MC str(12),CNM def(11) |
| 665 | 221 | NH ob1(74),CN tor1(53),$NC^{\alpha}$ tor(17) |
| 627 | 32 | CO ob1(68),M1 rock2(22) |
| 613 | 26 | CO ib1(34),MC str(19),CO ib2(11) |
| 598 | 3 | CO ob2(62),$CH_2$ rock(20),$NC^{\alpha}$ tor(16),$CH_2$ twist(10) |
| 545 | 115 | NH ob2(94),CN tor2(59) |
| 478 | 15 | MCN def(30),CO ib1(24),$C^{\alpha}CN$ def(17),M1 rock1(11) |
| 346 | 25 | CNM def(28),MCN def(27),CO ib2(21) |
| 279 | 2 | $NC^{\alpha}C$ def(19),CO ib1(12) |
| 234 | 10 | CNM def(30),$CNC^{\alpha}$ def(27),$C^{\alpha}CN$ def(25),MCN def(17) |

TABLE 6 (continued)

| $\nu$ ($cm^{-1}$) | $I^a$ | Potential energy distribution > 10% |
|---|---|---|
| 218 | 12 | $C^{\alpha}C$ tor(71),CN tor1(26),NH ob1(24),CN tor2(22),$NC^{\alpha}$ tor(16) |
| 189 | 0 | MC tor(21),CN tor2(20),CN tor1(14),NH ob2(12) |
| 173 | 0 | MC tor(87),CN tor2(11),NM tor(10) |
| 156 | 0 | NM tor(105) |
| 123 | 17 | $NC^{\alpha}$ tor(34),$C^{\alpha}C$ tor(26),CN tor1(19),NH ob1(17) |
| 111 | 16 | $CNC^{\alpha}$ def(34),$NC^{\alpha}C$ def(30),$C^{\alpha}CN$ def(24),MCN def(13) |
| 77 | 0 | $NC^{\alpha}$ tor(90),$C^{\alpha}C$ tor(70),MC tor(10) |
| | | *GLY7* |
| 3432 | 57 | NH str1(100) |
| 3363 | 135 | NH str2(99) |
| 3034 | 2 | CH10 str(70),CH11 str(31) |
| 3025 | 1 | MH1 str(85) |
| 2994 | 6 | MH19 str(74),MH18 str(21) |
| 2973 | 3 | MH3 str(51),MH2 str(47) |
| 2967 | 23 | MH18 str(38),MH17 str(37),CH11 str(15) |
| 2962 | 5 | CH11 str(53),CH10 str(21),MH18 str(13),MH17 str(10) |
| 2907 | 1 | MH2 str(46),MH3 str(38),MH1 str(15) |
| 2897 | 32 | MH17 str(47),MH18 str(29),MH19 str(23) |
| 1723 | 250 | CO str2(76),NH ib2(14) |
| 1689 | 145 | CO str1(73),NH ib1(13) |
| 1586 | 380 | NH ib2(69),CN str2(26) |
| 1544 | 268 | NH ib1(60),CN str1(27) |
| 1478 | 4 | M2 ab1(92) |
| 1457 | 5 | M2 ab2(95) |
| 1449 | 9 | M1 ab2(92) |
| 1437 | 6 | M1 ab1(52),$CH_2$ bend(44) |
| 1428 | 46 | $CH_2$ bend(53),M1 ab1(39) |
| 1416 | 4 | M2 sb(100) |
| 1366 | 34 | M1 sb(99) |
| 1331 | 31 | $CH_2$ wag(45),$C^{\alpha}C$ str(20),CN str2(19) |
| 1312 | 56 | $CH_2$ wag(35),CN str1(12),CN str2(11) |
| 1281 | 133 | CN str1(28),$CH_2$ wag(23),CO ib1(13),MC str(10) |
| 1236 | 28 | $CH_2$ twist(70) |
| 1170 | 3 | M2 rock1(64) |
| 1118 | 1 | M2 rock2(90) |
| 1111 | 12 | $NC^{\alpha}$ str(34),NM str(27),M1 rock1(11) |
| 1080 | 3 | NM str(26),$NC^{\alpha}$ str(21),$CH_2$ rock(13),M1 rock1(11) |
| 1053 | 25 | M1 rock2(68),CO ob1(18) |
| 1001 | 5 | $CH_2$ rock(24),M1 rock1(14),MC str(13),$C^{\alpha}C$ str(10) |
| 969 | 8 | M1 rock1(33),$NC^{\alpha}$ str(20),$CH_2$ rock(17) |
| 878 | 3 | $C^{\alpha}C$ str(17),CN str2(14) |
| 826 | 3 | $CH_2$ rock(32),MC str(15),CN str1(14) |
| 797 | 54 | CO ob2(43),$NC^{\alpha}C$ def(19) |
| 737 | 166 | NH ob2(56),CN tor2(46) |
| 634 | 50 | CO ob1(34),M1 rock2(11),NH ob1(11) |
| 617 | 18 | CO ob1(34),CO ib1(19),MC str(10) |

TABLE 6 (continued)

| $\nu$ ($cm^{-1}$) | $I^a$ | Potential energy distribution > 10% |
|---|---|---|
| 591 | 28 | CO ib1(18),$NC^{\alpha}$ tor(15),CO ob2(12),$C^{\alpha}C$ str(11),CO ob1(10) |
| 567 | 138 | NH ob1(113),CN tor1(83),$NC^{\alpha}$ tor(75) |
| 449 | 36 | CO ib1(26),MCN def(21),$C^{\alpha}CN$ def(16),$CH_2$ rock(15),CO ib2(13),$CNC^{\alpha}$ def(12) |
| 370 | 11 | MCN def(29),$C^{\alpha}CN$ def(28),CO ib2(27),$NC^{\alpha}$ tor(16) |
| 305 | 7 | $NC^{\alpha}C$ def(37),CNM def(16),CN tor1(12) |
| 269 | 12 | $NC^{\alpha}$ tor(34),$CNC^{\alpha}$ def(32),CNM def(31),$C^{\alpha}C$ tor(14),$C^{\alpha}CN$ def(11) |
| 220 | 5 | $CNC^{\alpha}$ def(48),$C^{\alpha}CN$ def(36),MCN def(19),CNM def(13) |
| 191 | 2 | NH ob2(35),CN tor1(25),CN tor2(21) |
| 173 | 0 | MC tor(107),$NC^{\alpha}$ tor(13) |
| 164 | 0 | NM tor(107) |
| 127 | 22 | $NC^{\alpha}$ tor(117),$C^{\alpha}C$ tor(13) |
| 104 | 2 | CN tor1(33),$NC^{\alpha}C$ def(27),NH ob1(15),$C^{\alpha}C$ tor(12) |
| 82 | 12 | $C^{\alpha}C$ tor(174),CN tor2(52),NH ob2(28) |

[a]Infrared intensity in km $mol^{-1}$.

In GLY7 the relations are reversed, consistent with the $N_{14}H_{15}$–$C_6O_5$ hydrogen bond. We also see that the free NH and CO bonds in each conformation have essentially the same force constants, 6.5 and 11.2 mdyn $Å^{-1}$, respectively, and that the $C_7$ hydrogen bond is stronger, as indicated by the larger differences between free and bonded NH and CO str force constants. The CO in-plane (ib) and out-of-plane (ob) bend force constants also show trends analogous to those exhibited by the stretch term, being slightly higher for the bonded CO group. The NH bend force constants do not show such clear trends: while increases in $f$(NH ib2) and $f$(NH ob2) from GLY5 to GLY7 are consistent with formation of the $C_7$ hydrogen bond, the decreases in $f$(NH ib1) and $f$(NH ob1) from GLY7 to GLY5 do not follow the expected pattern. From Table 1 it is significant that, of the bond angles, the $C_6N_7H_8$ angle shows the largest difference between the two conformations, increasing by 3.7° from GLY7 to GLY5 whereas the $C_{12}N_{14}H_{15}$ angle changes by only 1.3°. As Schäfer et al. [2] noted, this large increase favors the $C_5$ hydrogen bond interaction. Thus, it is likely that the decreases in $f$(NH ib1) and $f$(NH ob1) from GLY7 to GLY5 reflect the effect of the change in geometry, which more than compensates for the expected increases on formation of the $C_5$ hydrogen bond. Finally, no systematic changes can be discerned that can be unambiguously correlated with the non-planarity of the CONH groups in GLY7 [2]. For instance, both $f$(CN str1) and $f$(CN str2) are higher in GLY7 whereas non-planarity would be expected to reduce the CN bond orders.

In addition to the diagonal force constants, certain interaction terms show

instructive changes with hydrogen bonding. The free $f$(NH str–NH ib) is negligibly small in GLY5 and GLY7, but the bonded counterpart is large and of opposite signs in the two structures, $-0.11$ and 0.12 mdyn rad$^{-1}$, respectively. The strong dependence of the strength of a hydrogen bond on the H···O distance and the NH···O angle is well known [9]. In GLY5 a positive deformation of NH ib1 orients the NH bond more toward $O_{13}$, thereby increasing the hydrogen-bond strength and causing an increase in the NH bond length. In GLY7, on the other hand, an increase in NH ib2 moves $H_{15}$ away from $O_5$ and decreases the hydrogen-bond strength, leading to a decrease in the NH bond length. Similarly, $f$(NH str1–CO str2) has the value $-0.09$ mdyn Å$^{-1}$ in GLY5 but is negligible in GLY7, whereas $f$(NH str2–CO str1) is negligible in GLY5 but is as large as $-0.14$ mdyn Å$^{-1}$ in GLY7. The signs and relatively large magnitudes of these non-covalent interaction terms may be understood thus: the stretching of $N_7H_8$ in GLY5 or of $N_{14}H_{15}$ in GLY7 brings the hydrogen closer to the respective oxygen, increasing the hydrogen-bond strength and hence the CO bond length. These coupling force constants involving NH str, and several others in Tables 3 and 4, are not usually included in normal mode calculations; their direct effect on the frequencies is negligible because the NH str mixes little with the deformation and CO str coordinates. However, such terms may be important in molecular mechanics calculations of structure; they could be represented by analytical hydrogen-bond potential functions like the Lippincott–Schroeder potential [40].

In summary, our results on the CONH force constants confirm Schäfer et al.'s conclusion from their structural results of the significance of NH···OC interactions in GLY5 and GLY7 [2]. That the interaction in GLY7 is significant is not unexpected in view of the reasonably favorable H···O distance (2.058 Å) and NH···O angle (142°). It is remarkable, though, that the $C_5$ hydrogen bond in GLY5, with an NH···O angle of only 108°, can indeed have such effects on the CONH force constants.

We look next at the effects of the conformational change from GLY5 to GLY7. Of the diagonal terms, excluding those that we have already concluded are sensitive to the hydrogen bonds, significant changes are seen for $NC^{\alpha}$, $C^{\alpha}C$, CH10 and CH11 stretches; $CNC^{\alpha}$, $C^{\alpha}CN$ and $NC^{\alpha}C$ deformations (def); $CH_2$ rock; and CN and $NC^{\alpha}$ torsions (tor) — in other words, primarily the coordinates involving the $C^{\alpha}$ atom. Noteworthy are the small changes in the $CH_2$ bend, wag, and twist and the $C^{\alpha}C$ tor force constants. Among the off-diagonal terms, generally, significant changes are seen in interactions involving those same coordinates whose diagonal values are affected. Of course, the absence of planar symmetry in GLY7 results in non-zero interactions that vanish in GLY5; these couplings are mostly with $CH_2$ rock, NH ob1 and the torsions (NH ob2 is further removed from $C^{\alpha}$ than is NH ob1).

Unlike the CONH and $CH_2$ groups, affected mainly by hydrogen bonding and conformation, respectively, the $CH_3$ groups' diagonal force constants

change hardly at all from GLY5 to GLY7, with the minor exception of $f$(MH17 str). Even the MC and NM (M = methyl) stretches and torsions vary little. Furthermore, the interactions involving the methyl group coordinates also do not change significantly. These results are not unexpected because the conformations of the $CH_3$ groups remain the same. Of course, in structures where these groups have more conformational flexibility, their force fields will probably vary more. Within each conformation there are some differences within and between the $CH_3$ groups. The deformation force constants of $(N)CH_3$ are higher than those of $(C)CH_3$, and an in-plane CH str force constant is larger than an out-of-plane, in agreement with other ab initio work [41].

The results in Tables 3 and 4 therefore provide a guide as to which force constants in peptides are, or are not, sensitive to hydrogen bonding or conformation, and to the magnitudes of these variabilities. If more detailed variations with $\phi$ and $\psi$ are needed, one may use the large set of 4-21 relaxed geometries of glycine dipeptide derived by Klimkowski et al. [3] and compute only those group coordinate force constants that are expected to vary significantly.

To conclude this discussion of the ab initio force constants, we comment briefly on the diagonal cubic terms in Table 5. It has been found that cubic stretching force constants, at least, are quite reliably computed at the SCF level with a medium-size basis set [42,43]. The non-stretch terms are all small in magnitude and may be more susceptible to numerical errors. Most of the differences between GLY5 and GLY7 are small and may not be numerically significant. Noteworthy are the increases in both CO str terms which, however, do not seem relatable primarily to hydrogen bonding, and the CO ib and NH ib terms, all of which increase in magnitude on hydrogen bonding.

We turn now to the normal modes computed with the scaled force constants. The potential energy distributions (PEDs) are listed in Table 6 and the Cartesian displacements in the modes below 2000 $cm^{-1}$ are plotted in Figs. 2 and 3. For lack of space we have omitted from Fig. 2 the 77 $cm^{-1}$ torsional mode.

The modes above 500 $cm^{-1}$ are generally in the expected ranges for the amide, methylene and methyl group vibrations, showing that the scale factors, transferred and modified slightly from small amides [5] are reasonable. As with the force fields, we defer comparison with experimental data to a later section, and concentrate here on discussing the forms of the modes, their differences in GLY5 and GLY7, and indications of sensitivity to hydrogen bonding and conformation.

The well-localized NH str mode shows clearly the effect of hydrogen bonding. While the free NH str mode remains at 3431 $cm^{-1}$, the bonded NH str shifts down by 31 $cm^{-1}$ in GLY5 and by 68 $cm^{-1}$ in GLY7. The $CH_2$ stretches show surprising sensitivity to conformation, shifting up considerably in GLY7 and with an increase in their separation.

The amide I modes are seen, particularly in Figs. 2 and 3, to be largely CO str with smaller contributions from NH ib, contrary to what is derived from

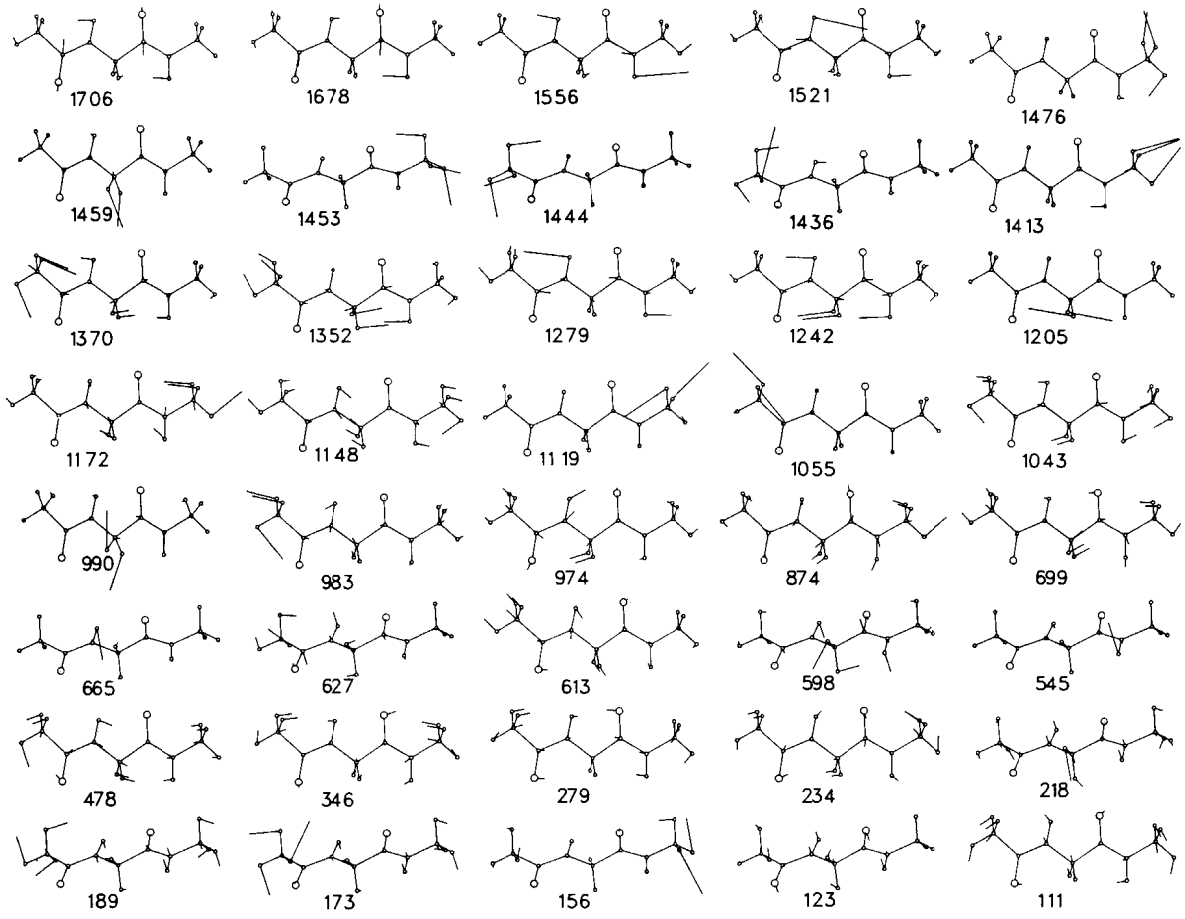


Fig. 2. Normal modes (below 2000 $cm^{-1}$) of GLY5. Oxygen atoms drawn extra large. Calculated frequencies in $cm^{-1}$ shown.

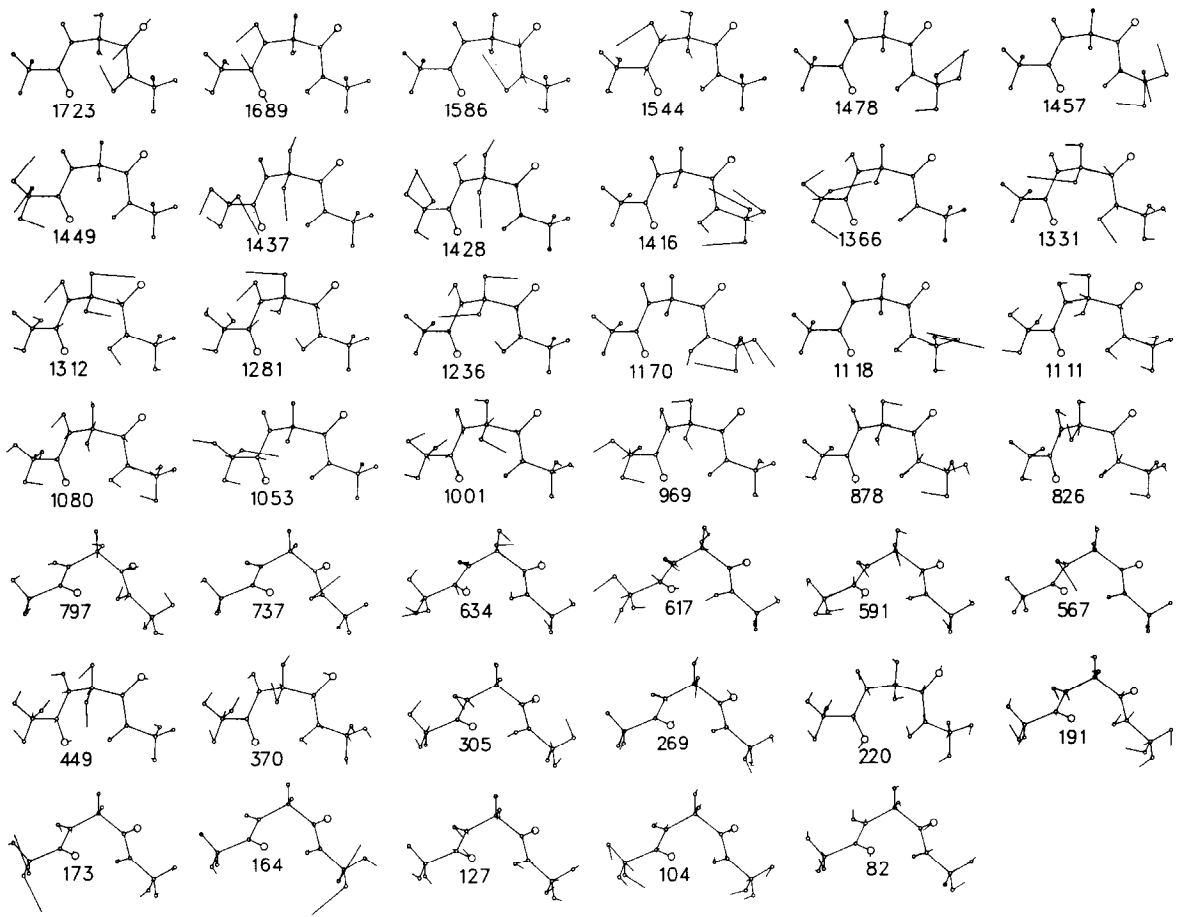


Fig. 3. Normal modes (below 2000 $cm^{-1}$) of GLY7. Oxygen atoms drawn extra large. Calculated frequencies in $cm^{-1}$ shown.

empirical force fields for polypeptides, which give a CN str component larger than the NH ib [11]. In GLY5 the symmetry of the structure and the near degeneracy result in the amide I modes being delocalized, with in-phase and out-of-phase vibrations of the two CONH groups. Because of the resulting possibility of coupling between the two CONH groups, the 28 $cm^{-1}$ splitting cannot be entirely attributed to hydrogen bonding. In GLY7, however, the amide I modes are localized, and much of the 35 $cm^{-1}$ separation arises from the different $f$(CO str) and $f$(NH ib) of the two groups.

The amide II PEDs resemble more closely those calculated for polypeptides [11]. Again, the GLY5 modes involve both CONH groups, and the higher frequency mode has a larger displacement of the free NH ib, contrary to expectation if hydrogen bonding were the only significant factor in causing the frequency splitting.

The $CH_2$ and $CH_3$ bend modes are quite pure vibrations with nearly the same frequencies in both structures, except where the more conformationally sensitive $CH_2$ bend shifts to near degeneracy with M1 ab1 in GLY7. The $CH_2$ wag mixes strongly with CN str and NH ib near 1300 $cm^{-1}$, making difficult identification of the amide III or its correlation with structure. Of the remaining modes above 400 $cm^{-1}$, the only ones that remain relatively invariant in GLY5 and GLY7 are the $CH_2$ twist, the methyl rocks at (frequencies in GLY5), 1172, 1119 and 1055 $cm^{-1}$, and quite unexpectedly the $C^{\alpha}C$ str at 874 $cm^{-1}$. In contrast with the $C^{\alpha}C$ str, the $NC^{\alpha}$ str at 1148 $cm^{-1}$ in GLY5 shifts to become mixed with NM str in the 1111 and 1080 $cm^{-1}$ modes in GLY7.

The amide V, which the PEDs show to be NH ob and CN tor vibrations, are well localized on each CONH group, and hence show shifts related to the $C_5$ and $C_7$ hydrogen bonds. The 665 $cm^{-1}$ mode in GLY5, mainly NH ob1, shifts down to 567 $cm^{-1}$ in GLY7 when the NH bond becomes free, whereas the free 545 $cm^{-1}$ mode in GLY5 becomes the bonded 737 $cm^{-1}$ mode in GLY7. That the free amide V in each structure is near 550 $cm^{-1}$, and that the splitting is twice as large in the $C_7$ hydrogen bond show the sensitivity of this mode to hydrogen-bond strength.

The modes involving CO ib and CO ob are highly mixed in the 400–800 $cm^{-1}$ region and the amide IV and VI cannot be readily identified. The exception is the CO ob2 vibration, forming the main contribution to modes at 598 $cm^{-1}$ in GLY5 and at 797 $cm^{-1}$ in GLY7. This large difference, which is also contrary to the effects of hydrogen bonding, can be explained thus: the free CO ob2 in GLY7 shifts upward in GLY5 where it becomes coupled to the $CH_2$ rock, which has shifted down on account of the conformational change, and this strong coupling gives rise to the 990 and 598 $cm^{-1}$ modes in GLY5.

Finally, of the skeletal and torsional modes below 400 $cm^{-1}$, only the methyl torsions at 173 and 156 $cm^{-1}$ in GLY5 remain largely unaltered in GLY7. Thus, aside from the $CH_3$ vibrations, most of the modes are quite different in GLY5 and GLY7 as a result of the changes in hydrogen bonding and conformation.

The highly localized NH str and NH ob modes show the best-defined changes with hydrogen bonding.

## DIPOLE MOMENT DERIVATIVES AND INTENSITIES

The dipole moment derivatives, $\partial\vec{\mu}/\partial S_i$, for GLY5 and GLY7, referred to the molecular axes [2], are listed in Table 7. The absolute intensities of the normal modes, shown in Table 6, are given by [44]

$$A_\alpha \text{ (km mol}^{-1}) = \frac{N_A \pi}{3c^2}\left(\frac{\partial\vec{\mu}}{\partial Q_\alpha}\right)^2 = 42.25\left(\frac{\partial\vec{\mu}}{\partial Q_\alpha}\right)^2$$

where the normal coordinate derivative for the $\alpha$th mode is $\partial\vec{\mu}/\partial Q_\alpha$ (D Å$^{-1}$ amu$^{-1/2}$) $= \sum_i L_{i\alpha}\dfrac{\partial\vec{\mu}}{\partial S_i}$ with $\mathbf{L}$ the eigenvector matrix, $\vec{\mathbf{S}} = \mathbf{L}\vec{\mathbf{Q}}$.

As with the force constants, we will try to relate changes in $\partial\vec{\mu}/\partial S_i$ to the hydrogen-bonding and conformational differences. To do so, it is illuminating to transform the derivatives with respect to the coordinates of each group to a common set of axes in the two structures. This has been done in Table 8. Thus, for instance, each CONH group in GLY5 and GLY7 is rotated so that the local $x$ axis is along CN and the local $z$ axis perpendicular to the CON plane. The local axes for the $CH_2$ and $CH_3$ groups are defined in Table 8. In this way, the directions as well as the magnitudes of the derivatives $\partial\vec{\mu}/\partial S_i$ are directly comparable between like groups. One can also see to what extent a $\partial\vec{\mu}/\partial S_i$ can be associated with a particular group and hence how transferable, in the context of the group moment model [14,45], are such derivatives. In the following $x$, $y$, and $z$ will refer to the local axes of the group under discussion.

As expected, the dipole derivatives of the NH and CO groups show changes that can be ascribed mainly to hydrogen-bonding differences. The NH str1 derivative is larger in GLY5 whereas the NH str2 derivative is larger in GLY7; the difference in the free NH str derivatives in the two structures may be due to substituent effects or conformational dependence, probably of the NH str1 which is adjacent to $C^\alpha$. Even more interesting are the directions of the NH str derivatives. The free NH str derivative is in each case at an angle of about 45° in the $x$–$y$ plane, i.e. at ~15° to the N–H bond. In GLY5 the bonded derivative is rotated to 26°, that is, toward $O_{13}$; and in GLY7 the NH str2 derivative is almost along $y$, in the direction of $O_5$. Stretching of a bonded NH in GLY5 or GLY7 simultaneously compresses the H···O distance. As we have seen [9], the H···O str dipole derivative is significant in magnitude and is oriented from O to H. Therefore, a bonded NH str derivative implicitly contains a contribution from the H···O str, which rotates the total derivative away from the approximately 45° angle of a free NH str derivative toward the H···O direction. This H···O contribution, as noted [9], also partly accounts for the increase

TABLE 7

Dipole moment derivatives $\partial\vec{\mu}/\partial S_i$ (in D Å$^{-1}$ or D rad$^{-1}$) with respect to molecular axes

| | GLY5 | | | | GLY7 | | | |
|---|---|---|---|---|---|---|---|---|
| | $\partial\mu_x/\partial S$ | $\partial\mu_y/\partial S$ | $\partial\mu_z/\partial S$ | $\lvert\partial\vec{\mu}/\partial S\rvert$ | $\partial\mu_x/\partial S$ | $\partial\mu_y/\partial S$ | $\partial\mu_z/\partial S$ | $\lvert\partial\vec{\mu}/\partial S\rvert$ |
| NH str1 | 0.12 | 1.02 | 0.0 | 1.03 | −0.30 | 0.94 | −0.01 | 0.98 |
| CO str1 | −1.49 | 6.05 | 0.0 | 6.23 | −2.37 | 5.82 | 0.18 | 6.29 |
| CN str1 | −2.16 | −4.26 | 0.0 | 4.77 | −1.77 | −3.52 | 0.22 | 3.94 |
| MC str | 0.38 | 0.36 | 0.0 | 0.52 | 0.49 | 0.32 | −0.02 | 0.58 |
| $NC^{\alpha}$ str | 1.65 | 0.62 | 0.0 | 1.76 | 2.77 | 0.28 | −0.20 | 2.79 |
| NH str2 | 0.42 | −0.33 | 0.0 | 0.53 | −1.06 | −0.50 | 1.03 | 1.56 |
| CO str2 | 4.69 | −4.28 | 0.0 | 6.35 | −2.84 | −4.88 | 2.01 | 5.98 |
| CN str2 | −4.64 | −0.02 | 0.0 | 4.64 | 0.75 | 3.50 | 1.02 | 3.72 |
| $C^{\alpha}C$ str | 0.39 | −0.05 | 0.0 | 0.40 | 0.60 | −0.67 | −0.95 | 1.31 |
| NM str | 1.34 | 2.88 | 0.0 | 3.18 | 1.16 | −0.40 | −2.72 | 2.98 |
| MH1 str | 0.38 | 0.06 | 0.0 | 0.38 | 0.27 | −0.08 | −0.04 | 0.28 |
| MH2 str | 0.07 | 0.09 | 0.18 | 0.21 | 0.08 | 0.00 | 0.13 | 0.15 |
| MH3 str | 0.07 | 0.09 | −0.18 | 0.21 | 0.10 | 0.00 | −0.23 | 0.25 |
| CH10 str | −0.18 | −0.27 | −0.11 | 0.34 | −0.10 | 0.09 | −0.24 | 0.27 |
| CH11 str | −0.18 | −0.27 | 0.11 | 0.34 | −0.18 | −0.38 | 0.02 | 0.42 |
| MH19 str | −0.55 | −0.25 | 0.0 | 0.60 | −0.06 | 0.32 | 0.31 | 0.46 |
| MH17 str | −0.24 | −0.30 | 0.28 | 0.48 | 0.17 | 0.02 | 0.57 | 0.60 |
| MH18 str | −0.24 | −0.30 | −0.28 | 0.48 | −0.50 | 0.18 | 0.25 | 0.59 |
| MCN def | −1.63 | −1.41 | 0.0 | 2.15 | −1.83 | −0.74 | 0.30 | 1.99 |
| CO ib1 | −3.37 | −1.46 | 0.0 | 3.67 | −3.51 | −1.17 | 0.50 | 3.73 |
| $CNC^{\alpha}$ def | 3.27 | 2.68 | 0.0 | 4.22 | 4.03 | 0.58 | −0.46 | 4.10 |
| NH ib1 | 0.82 | 0.57 | 0.0 | 1.00 | 0.39 | 0.36 | −0.07 | 0.54 |
| $C^{\alpha}CN$ def | 1.14 | 1.34 | 0.0 | 1.76 | 1.65 | 0.38 | −2.42 | 2.95 |
| CO ib2 | −3.02 | −2.65 | 0.0 | 4.02 | −0.91 | 1.41 | 2.65 | 3.13 |
| CNM def | 0.74 | −0.26 | 0.0 | 0.78 | −0.56 | −1.19 | 0.29 | 1.35 |
| NH ib2 | 0.55 | 0.16 | 0.0 | 0.58 | 0.35 | −0.53 | −0.52 | 0.82 |
| M1 sb | 0.43 | −0.15 | 0.0 | 0.46 | 0.44 | −0.12 | 0.0 | 0.45 |
| M1 ab1 | −0.05 | −0.37 | 0.0 | 0.38 | −0.04 | −0.35 | 0.02 | 0.35 |
| M1 ab2 | 0.0 | 0.0 | 0.46 | 0.46 | 0.01 | 0.01 | 0.45 | 0.45 |
| M1 rock1 | 0.11 | 0.21 | 0.0 | 0.24 | 0.07 | 0.14 | −0.01 | 0.15 |
| M1 rock2 | 0.0 | 0.0 | 0.25 | 0.25 | 0.0 | 0.00 | 0.18 | 0.18 |
| $NC^{\alpha}C$ def | −3.75 | −2.79 | 0.0 | 4.68 | 0.67 | −0.40 | −0.75 | 1.08 |
| $CH_2$ bend | −0.01 | 0.40 | 0.0 | 0.40 | −0.26 | 0.02 | −0.35 | 0.44 |
| $CH_2$ wag | −0.13 | 0.22 | 0.0 | 0.26 | 0.07 | 0.07 | −0.10 | 0.14 |
| $CH_2$ twist | 0.0 | 0.0 | −1.46 | 1.46 | −0.71 | 0.24 | −1.28 | 1.49 |
| $CH_2$ rock | 0.0 | 0.0 | −0.34 | 0.34 | −3.18 | 0.19 | 2.15 | 3.84 |
| M2 sb | −0.05 | −0.02 | 0.0 | 0.05 | −0.02 | −0.07 | 0.06 | 0.09 |
| M2 ab1 | 0.34 | −0.09 | 0.0 | 0.36 | −0.06 | −0.34 | 0.00 | 0.35 |
| M2 ab2 | 0.0 | 0.0 | 0.31 | 0.31 | 0.28 | −0.07 | 0.12 | 0.31 |
| M2 rock1 | −0.01 | 0.05 | 0.0 | 0.05 | 0.05 | 0.00 | −0.08 | 0.10 |
| M2 rock2 | 0.0 | 0.0 | 0.07 | 0.07 | 0.08 | 0.03 | 0.11 | 0.14 |
| CO ob1 | 0.0 | 0.0 | 0.78 | 0.78 | −0.09 | −0.15 | 1.60 | 1.61 |
| NH ob1 | 0.0 | 0.0 | 2.45 | 2.45 | 0.00 | 0.28 | 1.03 | 1.07 |
| CO ob2 | 0.0 | 0.0 | −0.95 | 0.95 | 0.13 | 0.0 | 0.46 | 0.48 |

TABLE 7 (continued)

| | GLY5 | | | | GLY7 | | | |
|---|---|---|---|---|---|---|---|---|
| | $\partial\mu_x/\partial S$ | $\partial\mu_y/\partial S$ | $\partial\mu_z/\partial S$ | $\lvert\partial\vec{\mu}/\partial S\rvert$ | $\partial\mu_x/\partial S$ | $\partial\mu_y/\partial S$ | $\partial\mu_z/\partial S$ | $\lvert\partial\vec{\mu}/\partial S\rvert$ |
| NH ob2 | 0.0 | 0.0 | −2.22 | 2.22 | −2.31 | 0.76 | −1.10 | 2.67 |
| MC tor | 0.0 | 0.0 | −0.18 | 0.18 | −0.01 | −0.02 | −0.18 | 0.18 |
| CN tor1 | 0.0 | 0.0 | −3.50 | 3.50 | 0.61 | 0.27 | −3.39 | 3.45 |
| $NC^{\alpha}$ tor | 0.0 | 0.0 | −3.16 | 3.16 | 0.77 | −0.18 | −5.02 | 5.09 |
| $C^{\alpha}C$ tor | 0.0 | 0.0 | −3.34 | 3.34 | −4.11 | 0.93 | −1.63 | 4.52 |
| CN tor2 | 0.0 | 0.0 | 0.03 | 0.03 | 0.17 | 0.14 | 0.66 | 0.69 |
| NM tor | 0.0 | 0.0 | −0.18 | 0.18 | −0.20 | −0.01 | −0.08 | 0.21 |

in intensity of a bonded NH str mode. Thus, the magnitudes and directions of the NH str derivatives show clearly the presence of NH···O interactions in GLY5 and GLY7. Furthermore, as found previously [9], in hydrogen-bonded NH groups the transition moment direction of the NH str mode can vary considerably with the NH···O angle.

The CO str derivatives also have magnitude changes consistent with hydrogen-bonding effects; the small variation in the directions, compared to that of the NH str derivatives, is not surprising in view of the much smaller modulation of the O···H distance by a CO str and the much larger magnitude of the CO derivative. Similarly, the magnitudes of the NH and CO bend derivatives can all be correlated with the $C_5$ and $C_7$ hydrogen bonds, that is, in each structure the bonded derivative is larger than the free. Of course, part of the changes may be due to the conformation; this is expected to be more likely for the derivatives of the NH and CO groups adjacent to $C^{\alpha}$. All the CN str derivatives have the same orientation, with larger magnitudes in GLY5, and are not readily related to hydrogen bonding. A very large difference is seen in the CN tor derivatives in the two conformations.

Not surprisingly, the stretch and deformation derivatives at $C^{\alpha}$ are significantly different in the two conformations. Particularly large magnitude changes are seen in the $NC^{\alpha}$ str, $C^{\alpha}C$ str, $NC^{\alpha}C$ def, and $CH_2$ rock derivatives; and although the magnitudes are more similar in GLY5 and GLY7, of the other derivatives, their directions with respect to the $NC^{\alpha}C$ axes change, some drastically. For instance, in GLY5 the $CH_2$ twist, $NC^{\alpha}$ tor and $C^{\alpha}C$ tor (as well as the $CH_2$ rock) derivatives are, by symmetry, in the $z$ direction, perpendicular to $NC^{\alpha}C$. In GLY7, however, these derivatives are mainly in the $x$–$y$ plane. We may understand these directional changes by looking at the $NC^{\alpha}$ tor and $C^{\alpha}C$ tor derivatives resolved not along the $NC^{\alpha}C$ local axes, but along the adjacent CONH local axes: the derivatives remain predominantly along $z$ in GLY7. Thus, the $NC^{\alpha}$ tor and $C^{\alpha}C$ tor derivatives are more characteristic of the CONH groups and probably owe their large magnitudes to these more polar groups.

TABLE 8

Dipole moment derivatives $\partial\vec{\mu}/\partial S_i$ (in D Å$^{-1}$ or D rad$^{-1}$) with respect to group axes[a]

| | $\partial\mu_x/\partial S$ | $\partial\mu_y/\partial S$ | $\partial\mu_z/\partial S$ | $\lvert\partial\vec{\mu}/\partial S\rvert$ | $\theta$[b] |
|---|---|---|---|---|---|
| *C6 N7 O5* | | | | | |
| NH str1 | 0.93 | 0.44 | 0.0 | 1.03 | 26 |
| | 0.65 | 0.73 | −0.01 | 0.98 | 48 |
| CO str1 | 4.34 | 4.47 | 0.0 | 6.23 | 46 |
| | 3.82 | 4.99 | 0.15 | 6.29 | 53 |
| CN str1 | −4.76 | −0.42 | 0.0 | 4.77 | −175 |
| | −3.93 | −0.25 | 0.15 | 3.94 | −176 |
| MC str | 0.50 | −0.13 | 0.0 | 0.52 | −15 |
| | 0.52 | −0.26 | −0.01 | 0.58 | −26 |
| NC$^{\alpha}$ str | 1.40 | −1.07 | 0.0 | 1.76 | −38 |
| | 1.64 | −2.25 | −0.13 | 2.79 | −54 |
| MCN def | −2.06 | 0.63 | 0.0 | 2.15 | 163 |
| | −1.57 | 1.21 | 0.25 | 1.99 | 142 |
| CO ib1 | −3.02 | 2.09 | 0.0 | 3.67 | 145 |
| | −2.79 | 2.44 | 0.39 | 3.73 | 139 |
| CNC$^{\alpha}$ def | 4.00 | −1.35 | 0.0 | 4.22 | −19 |
| | 2.55 | −3.19 | −0.34 | 4.10 | −51 |
| NH ib1 | 0.92 | −0.39 | 0.0 | 1.00 | −23 |
| | 0.51 | −0.16 | −0.06 | 0.54 | −17 |
| CO ob1 | 0.0 | 0.0 | 0.78 | 0.78 | 0 |
| | −0.21 | 0.04 | 1.60 | 1.61 | 170 |
| NH ob1 | 0.0 | 0.0 | 2.45 | 2.45 | 0 |
| | 0.22 | 0.16 | 1.03 | 1.07 | 36 |
| MC tor | 0.0 | 0.0 | −0.18 | 0.18 | 0 |
| | −0.02 | −0.01 | −0.18 | 0.18 | −153 |
| CN tor1 | 0.0 | 0.0 | −3.50 | 3.50 | 0 |
| | 0.61 | −0.46 | −3.37 | 3.45 | −37 |
| NC$^{\alpha}$ tor | 0.0 | 0.0 | −3.16 | 3.16 | 0 |
| | 0.33 | −0.87 | −5.00 | 5.09 | −69 |
| *C12 N14 O13* | | | | | |
| NH str2 | 0.39 | 0.37 | 0.0 | 0.53 | 43 |
| | 0.19 | 1.50 | 0.39 | 1.56 | 83 |
| CO str2 | 4.28 | 4.69 | 0.0 | 6.35 | 48 |
| | 4.06 | 4.38 | 0.43 | 5.98 | 47 |
| CN str2 | −4.62 | −0.40 | 0.0 | 4.64 | −175 |
| | −3.69 | −0.49 | −0.17 | 3.72 | −173 |
| C$^{\alpha}$C str | 0.39 | 0.08 | 0.0 | 0.40 | 12 |
| | 0.90 | −0.89 | −0.32 | 1.31 | −45 |
| NM str | 1.60 | −2.75 | 0.0 | 3.18 | −60 |
| | 1.25 | −2.71 | −0.04 | 2.98 | −65 |
| C$^{\alpha}$CN def | 1.26 | −1.23 | 0.0 | 1.76 | −44 |
| | 0.36 | −2.90 | −0.38 | 2.95 | −83 |
| CO ib2 | −3.24 | 2.37 | 0.0 | 4.02 | 144 |
| | −2.18 | 2.24 | 0.10 | 3.13 | 134 |
| CNM def | 0.71 | 0.32 | 0.0 | 0.78 | 24 |
| | 1.06 | 0.84 | 0.07 | 1.35 | 39 |

TABLE 8 (continued)

| | $\partial\mu_x/\partial S$ | $\partial\mu_y/\partial S$ | $\partial\mu_z/\partial S$ | $\lvert\partial\vec{\mu}/\partial S\rvert$ | $\theta^b$ |
|---|---|---|---|---|---|
| *C12 N14 O13* | | | | | |
| NH ib2 | 0.57 | −0.11 | 0.0 | 0.58 | −11 |
| | 0.64 | −0.46 | −0.24 | 0.82 | −35 |
| CO ob2 | 0.0 | 0.0 | 0.95 | 0.95 | 0 |
| | −0.18 | 0.33 | −0.30 | 0.48 | 119 |
| NH ob2 | 0.0 | 0.0 | 2.22 | 2.22 | 0 |
| | −0.06 | −0.06 | 2.67 | 2.67 | −137 |
| $C^{\alpha}C$ tor | 0.0 | 0.0 | 3.34 | 3.34 | 0 |
| | 0.16 | 0.29 | 4.51 | 4.52 | 60 |
| CN tor2 | 0.0 | 0.0 | −0.03 | 0.03 | 0 |
| | −0.39 | 0.43 | −0.38 | 0.69 | 132 |
| NM tor | 0.0 | 0.0 | 0.18 | 0.18 | 0 |
| | 0.06 | 0.03 | 0.20 | 0.21 | 28 |
| *N7 C9 C12* | | | | | |
| $NC^{\alpha}$ str | 1.63 | −0.67 | 0.0 | 1.76 | −22 |
| | 2.77 | −0.19 | −0.25 | 2.79 | −4 |
| $C^{\alpha}C$ str | 0.40 | 0.03 | 0.0 | 0.40 | 5 |
| | 0.58 | −1.04 | 0.53 | 1.31 | −61 |
| CH10 str | −0.17 | 0.28 | 0.11 | 0.34 | 121 |
| | −0.10 | −0.22 | −0.13 | 0.27 | −115 |
| CH11 str | −0.17 | 0.28 | −0.11 | 0.34 | 121 |
| | −0.19 | −0.04 | 0.37 | 0.42 | −169 |
| $CNC^{\alpha}$ def | 3.18 | −2.78 | 0.0 | 4.22 | −41 |
| | 4.04 | −0.42 | −0.56 | 4.10 | −6 |
| $C^{\alpha}CN$ def | 1.10 | −1.38 | 0.0 | 1.76 | −51 |
| | 1.63 | −2.36 | −0.69 | 2.95 | −55 |
| $NC^{\alpha}C$ def | −3.66 | 2.91 | 0.0 | 4.68 | 142 |
| | 0.66 | −0.80 | 0.31 | 1.08 | −51 |
| $CH_2$ bend | −0.02 | −0.40 | 0.0 | 0.40 | −94 |
| | −0.26 | −0.34 | −0.07 | 0.44 | −128 |
| $CH_2$ wag | −0.14 | −0.22 | 0.0 | 0.26 | −123 |
| | 0.07 | −0.09 | −0.09 | 0.14 | −52 |
| $CH_2$ twist | 0.0 | 0.0 | 1.46 | 1.46 | 0 |
| | −0.72 | −1.23 | −0.44 | 1.49 | −120 |
| $CH_2$ rock | 0.0 | 0.0 | 0.34 | 0.34 | 0 |
| | −3.15 | 2.20 | 0.06 | 3.84 | 145 |
| $NC^{\alpha}$ tor | 0.0 | 0.0 | 3.16 | 3.16 | 0 |
| | 0.73 | −5.01 | −0.52 | 5.09 | −82 |
| $C^{\alpha}C$ tor | 0.0 | 0.0 | 3.34 | 3.34 | 0 |
| | −4.11 | −1.43 | −1.24 | 4.52 | −161 |
| *C4 C6 H1* | | | | | |
| MC str | 0.33 | 0.40 | 0.0 | 0.52 | 50 |
| | 0.45 | 0.36 | −0.00 | 0.58 | 39 |
| MH1 str | 0.36 | 0.11 | 0.0 | 0.38 | 17 |
| | 0.28 | −0.05 | −0.03 | 0.28 | −11 |

TABLE 8 (continued)

| | $\partial\mu_x/\partial S$ | $\partial\mu_y/\partial S$ | $\partial\mu_z/\partial S$ | $\lvert\partial\vec{\mu}/\partial S\rvert$ | $\theta^b$ |
|---|---|---|---|---|---|
| *C4 C6 H1* | | | | | |
| MH2 str | 0.06 | 0.10 | 0.18 | 0.21 | 59 |
| | 0.08 | 0.01 | 0.13 | 0.15 | 6 |
| MH3 str | 0.06 | 0.10 | −0.18 | 0.21 | 59 |
| | 0.11 | 0.02 | −0.22 | 0.25 | 11 |
| MCN def | −1.44 | −1.60 | 0.0 | 2.15 | −132 |
| | −1.76 | −0.91 | 0.23 | 1.99 | −153 |
| M1 sb | 0.44 | −0.10 | 0.0 | 0.46 | −13 |
| | 0.45 | −0.08 | 0.01 | 0.45 | −10 |
| M1 ab1 | −0.00 | −0.38 | 0.0 | 0.38 | −91 |
| | −0.01 | −0.35 | 0.01 | 0.35 | −92 |
| M1 ab2 | 0.0 | 0.0 | 0.46 | 0.46 | 0 |
| | −0.00 | −0.01 | 0.45 | 0.46 | −119 |
| M1 rock1 | 0.09 | 0.23 | 0.0 | 0.24 | 69 |
| | 0.06 | 0.14 | −0.00 | 0.15 | 67 |
| M1 rock2 | 0.0 | 0.0 | 0.25 | 0.25 | 0 |
| | −0.00 | −0.00 | 0.18 | 0.18 | −154 |
| MC tor | 0.0 | 0.0 | −0.18 | 0.18 | 0 |
| | 0.0 | −0.02 | −0.18 | 0.18 | −89 |
| *N16 C14 H19* | | | | | |
| NM str | −3.18 | 0.02 | 0.0 | 3.18 | 180 |
| | −2.97 | 0.27 | −0.09 | 2.98 | 175 |
| MH19 str | 0.45 | 0.39 | 0.0 | 0.60 | 41 |
| | 0.38 | 0.25 | 0.00 | 0.46 | 34 |
| MH17 str | 0.37 | 0.09 | −0.28 | 0.48 | 13 |
| | 0.47 | −0.01 | −0.37 | 0.60 | −2 |
| MH18 str | 0.37 | 0.09 | 0.28 | 0.48 | 13 |
| | 0.44 | 0.00 | 0.40 | 0.59 | 1 |
| CNM def | −0.08 | −0.78 | 0.0 | 0.78 | −96 |
| | 0.19 | −1.33 | 0.15 | 1.35 | −82 |
| M2 sb | 0.04 | 0.03 | 0.0 | 0.05 | 41 |
| | 0.04 | −0.08 | −0.02 | 0.09 | −62 |
| M2 ab1 | −0.06 | −0.35 | 0.0 | 0.36 | −100 |
| | −0.05 | −0.34 | −0.02 | 0.35 | −99 |
| M2 ab2 | 0.0 | 0.0 | −0.31 | 0.31 | 0 |
| | −0.01 | −0.01 | −0.31 | 0.31 | −127 |
| M2 rock1 | −0.04 | 0.03 | 0.0 | 0.05 | 144 |
| | −0.10 | 0.03 | −0.02 | 0.10 | 162 |
| M2 rock2 | 0.0 | 0.0 | −0.07 | 0.07 | 0 |
| | 0.08 | 0.03 | −0.11 | 0.14 | 23 |
| NM tor | 0.0 | 0.0 | 0.18 | 0.18 | 0 |
| | −0.00 | −0.05 | 0.20 | 0.21 | −95 |

[a]Local axes of group A B C defined thus: $\hat{x}$ = AB, $\hat{z}$ = AC **X** AB. Entries are for GLY5 (first line) and GLY7 (second line). [b]Angle from $\hat{x}$ in $x$-$y$ plane, in degrees.

The sizable $CH_2$ twist and rock derivatives are probably also affected by the presence of the CONH groups.

In the $CH_3$ groups, the CH str and $CH_3$ def derivatives remain largely the same in magnitude and direction in GLY5 and GLY7, as do the derivatives of MC and NM stretches and torsions. Between the two methyl groups, however, there are differences.

Finally, the derivatives for the amide groups can be compared with the 3-21G derivatives of comparable coordinates that we previously computed for isolated *N*-methylacetamide [14]; this is readily done because the local CONH axes are oriented similarly. The magnitudes for GLY5 and *N*-methylacetamide, respectively, are as follows (direction in degrees from *x*-axis in parentheses): CO str1 = 6.23(46), 5.58(47); CN str1 = 4.77(−175), 3.72(−178); NH str2 = 0.53(43), 0.70(61); CO ib1 = 3.67(145), 2.93(144); NH ib2 = 0.58(−11), 0.55(11); CO ob1 = 0.78, 0.45; NH ob2 = 2.22, 2.02; CN tor2 = 0.03, 0.27. The reasonably good agreement in magnitude and direction between most of the derivatives, given the different basis sets, CONH geometries, and hydrogen bonding, shows that the CONH derivatives are characteristic of the peptide group and are therefore, to a first approximation, transferable. This further supports the essential validity of the group moment model [45] as an alternative to the bond moment model [44] in calculating infrared intensities.

The infrared intensities are given in Table 6. The intensities can have more complex dependences on structure than the group coordinate derivatives because the normal coordinate derivatives require, in addition to $\partial\vec{\mu}/\partial S_i$, the eigenvectors, which in turn are also structure-dependent through the **F** and **B** matrices. In a symmetric system like GLY5, moreover, where some normal modes may be delocalized, one has to take into account the vectorial sum of contributions to $\partial\vec{\mu}/\partial Q_\alpha$ from more than one chemical group. Intensities therefore place more stringent requirements on the accuracy of an ab initio calculation than do structures, force constants, or internal coordinate dipole derivatives.

The NH str modes are highly localized and their intensities reflect the effects of hydrogen bonding, being higher the stronger the hydrogen bond. The $(N)CH_3$ stretches are seen to be more intense than their $(C)CH_3$ counterparts. The amide I and II are the most intense modes. The delocalized nature of amide I in GLY5, with in-phase and out-of-phase vibrations of the CONH groups, results in the in-phase mode having a much smaller intensity because of partial cancellation of the contributions from the two groups to the transition moment. A similar effect also occurs for the amide II. The more localized amide I and II in GLY7 are all intense. The lower frequency amide I is weaker than the higher frequency mode, showing that, at least in such weak hydrogen-bonding systems, it can be difficult to assign bands on the basis of hydrogen-bonding considerations if the intensities depend on several contributions, some of which can vary with conformation as well as hydrogen bonding. In such cases it is

clearly important to compute intensities using reliable force fields and dipole derivatives.

We should comment on the relative intensities of the amide I and II modes. Our results give a lower total integrated intensity for the two amide I modes than for the amide II pair, the ratio $A_I/A_{II}$ being 0.56 in GLY5 and 0.61 in GLY7, and the strongest band in each conformation is an amide II. These are contrary to expectation. In previous work [14] on *N*-methylacetamide our 3-21G dipole derivatives, together with various empirical force fields, also gave intensity ratios significantly less than unity, ranging from 0.38 to 0.73 for the isolated molecule. Thus, the calculated intensity ratio is very sensitive to the amide I and II eigenvectors. We found [14] that this ratio is improved if the amide I has more CN str and less NH ib contributions, and if in the amide II the CO str component is in phase with the CN str. Our GLY5 and GLY7 force fields yield very little CN str contribution to amide I and the CO str and CN str components in amide II are out of phase. We cannot be sure at present whether the deficiencies in GLY5 and GLY7 lie mainly in the eigenvectors or are also in the dipole derivatives.

In the CH bend region, the $CH_2$ bend and $(C)CH_3$ bends are the most intense; the latter are stronger than the $(N)CH_3$ bends, in contrast to the $CH_3$ stretches. The amide III modes are also strong but the complicated mixings make difficult any correlation with hydrogen bonding or conformation alone. All the other modes are weak except for the amide V; these relatively well-localized NH ob vibrations are stronger for the bonded NH group, as expected.

## COMPARISON WITH EXPERIMENT

Our results are now compared with available experimental force fields and spectra. There are no spectroscopic data specifically on isolated glycine dipeptide known to be in the $C_5$ or $C_7$ conformation used in our calculations, and no force field has been refined for glycine dipeptide. The comparisons will therefore necessarily be indirect and incomplete.

Table 4 lists, alongside the GLY5 and GLY7 force constants, the values of comparable terms in force fields refined for the CONH and $CH_2$ groups in polyglycine I (PGI) [46] and in glycylglycine (Gly-Gly) [47]; in the Gly-Gly set, we have transformed the out-of-plane and torsion terms to conform to our coordinate definitions. Also shown are force constants for $CH_2$ and $CH_3$ groups refined for alkanes [48], the comparison being made taking the NH and CO groups in glycine dipeptide to be $CH_2$ units. Several other refined force fields for these groups are available, but these three should be representative and sufficient for our present purposes.

The PGI force field was refined to solid state data using a model with $(\phi,\psi) = (-149.9°, 146.5°)$, and in a redundant primitive internal coordinate basis with many terms kept fixed or set to zero. The Gly-Gly field was also

refined to solid state data. Even so, the comparison shows close agreement among the force fields for many of the terms, though of course the ab initio fields are more complete.

Table 9 compares our calculated frequencies for the peptide group modes with infrared data on matrix-isolated glycine dipeptide [21]. We have omitted the amide V modes, because the observed data [21] are not given in sufficient detail to permit a clear-cut assignment, as well as the less reliably assigned amide IV and VI modes. By comparison with the spectra of the compounds $CH_3CONHCH_2CON(C_2H_5)_2$ and $CH_3CON(CH_3)CH_2CONHC_2H_5$, which can form intramolecular hydrogen bonds only of the $C_5$ or $C_7$ type, respectively, Grenie et al. [21] assigned the amide modes in glycine dipeptide to a mixture of $C_5$ and $C_7$ conformations. Considering that the exact conformations are not known and may in any case be different from those used in our calculations, the comparison is necessarily suggestive only. Grenie et al. have also given assignments for many of the skeletal and CH modes. Each can be matched with a calculated mode of either GLY5 or GLY7, but we will not attempt a detailed comparison at this time in view of the incompleteness of the experimental data.

For the NH stretches, the calculated separations between free and bonded frequencies are just over half of those observed, although the computed GLY5

TABLE 9

Comparison of some observed and calculated amide mode frequencies[a]

| | Observed[b] | Calculated | |
|---|---|---|---|
| | | GLY5 | GLY7 |
| NH stretch | 3484s | 3431(23) | 3432(57) |
| | 3428s | 3400(71) | |
| | 3365s | | 3363(135) |
| Amide I | 1707s | | 1723(250) |
| | | 1706(24) | |
| | 1693s | 1678(444) | |
| | 1683m | | 1689(145) |
| Amide II | 1553s | | 1586(380) |
| | 1516s | 1556(206) | |
| | ~1510s | | 1544(268) |
| | 1504s | 1521(634) | |
| Amide III | 1349m | 1352(121) | 1331(31) |
| | 1288w | | 1312(56) |
| | 1271w | 1279(1) | 1281(133) |
| | 1246w | 1242(106) | |

[a]Frequencies in $cm^{-1}$. Calculated infrared intensities in km $mol^{-1}$ in parentheses. [b]Ref. 21.

splitting of 31 $cm^{-1}$ is in better agreement with the dilute solution value [18] of 34 $cm^{-1}$. The calculated amide I intensities, showing one GLY5 mode to be weak, are consistent with the observation of only three bands in the spectrum. The calculated amide II intensities indicate that four bands should be observed, and this is the case; we agree with the proposed [21] assignments for the $C_7$ structure, but our calculations indicate that the suggested assignments [21] for the $C_5$ structure should be reversed. The amide III modes, usually associated with NH ib plus CN str, are in fact typically mixed with $C^{\alpha}$ modes [11], in the present case mainly with $CH_2$ wag. If we include such modes above 1300 $cm^{-1}$ to which NH ib contributes (see Figs. 2 and 3), and which are therefore sensitive to N-deuteration, the calculations account reasonably well for the observed bands. Our calculations thus strongly support the empirically-based conclusion [21] that the $C_5$ and $C_7$ conformations are both present in the matrix-isolated sample. A more detailed re-examination of the spectra may be useful in the light of our calculations.

## CONCLUSIONS

Our results on glycine dipeptide in $C_5$ and $C_7$ conformations with intramolecular hydrogen bonding complement and extend previous ab initio studies [6–8] of the force field of the isolated peptide group in *N*-methylacetamide, and should provide a firm basis for empirical vibrational analyses of polypeptides [11]. Similar calculations on alanine dipeptide will be reported in the near future.

Together with the extensive work on geometry optimization by Schäfer and coworkers [2,3] our results show the feasibility of force field calculations with extended basis sets on biologically important molecules as large as dipeptides. Because this level of ab initio theory is still inadequate for force constants, it is encouraging that the scale factors transferred from small amides [5] yield reasonably good results, thus further showing the effectiveness of the scaled quantum mechanical approach [4].

## ACKNOWLEDGMENT

This research was supported by NSF grants DMB-8517812 and DMR-8303610. We thank The University of Michigan Computing Center for a generous special allocation of computing funds.

## REFERENCES

1 B. Pullman and A. Pullman, Adv. Protein Chem., 23 (1974) 283.
2 L. Schäfer, C. Van Alsenoy, and J.N. Scarsdale, J. Chem. Phys., 76 (1982) 1439.

3 V.J. Klimkowski, L. Schäfer, F.A. Momany, and C. Van Alsenoy, J. Mol. Struct. (Theochem), 124 (1985) 143.
4 G. Fogarasi and P. Pulay, Ann. Rev. Phys. Chem., 35 (1984) 191.
5 G. Fogarasi and A. Balázs, J. Mol. Struct. (Theochem), 133 (1985) 105.
6 Y. Sugawara, A.Y. Hirakawa, and M. Tsuboi, J. Mol. Spectrosc., 108 (1984) 206.
7 Y. Sugawara, A.Y. Hirakawa, M. Tsuboi, S. Kato, and K. Morokuma, J. Mol. Spectrosc., 115 (1986) 21.
8 A. Balázs, J. Mol. Struct. (Theochem), 153 (1987) 103.
9 T.C. Cheam and S. Krimm, J. Mol. Struct., 146 (1986) 175.
10 T.C. Cheam and S. Krimm, Spectrochim. Acta, Part A, 44 (1988) 185.
11 S. Krimm and J. Bandekar, Adv. Protein Chem., 38 (1986) 181.
12 K. Siam, V.J. Klimkowski, C. Van Alsenoy, J.D. Ewbank and L. Schäfer, J. Mol. Struct. (Theochem), 152 (1987) 261.
13 U. Berkert and N.L. Allinger, Molecular Mechanics, American Chemical Society, Washington, DC, 1982.
14 T.C. Cheam and S. Krimm, J. Chem. Phys., 82 (1985) 1631.
15 M. Tsuboi, T. Shimanouchi, and S. Mizushima, J. Am. Chem. Soc., 81 (1959) 1406.
16 M. Avignon, P.V. Huong, J. Lascombe, M. Marraud, and J. Néel, Biopolymers, 8 (1969) 69.
17 J. Néel, Pure Appl. Chem., 31 (1972) 201.
18 F.R. Maxfield, S.J. Leach, E.R. Stimson, S.P. Powers, and H.A. Scheraga, Biopolymers, 18 (1979) 2507.
19 I.M. Ginzburg, J. Gen. Chem., 52 (1982) 1445.
20 C.I. Jose, A.A. Belhekar, and M.S. Agashe, Biopolymers, 26 (1987) 1315.
21 Y. Grenie, M. Avignon, and C. Garrigou-Lagrange, J. Mol. Struct., 24 (1975) 293.
22 Y. Koyama and T. Shimanouchi, Biopolymers, 6 (1968) 1037.
23 M. Avignon, C. Garrigou-Lagrange, and P. Botherel, Biopolymers, 12 (1973) 1651.
24 IUPAC-IUB Commission on Biochemical Nomenclature, Biochemistry, 9 (1970) 3471.
25 P. Pulay, G. Fogarasi, F. Pang, and J.E. Boggs, J. Am. Chem. Soc., 101 (1979) 2550.
26 B.A. Hess, Jr., L.J. Schaad, P. Cársky, and R. Zahradník, Chem. Rev., 86 (1986) 709.
27 IUPAC Commission on Molecular Structure and Spectroscopy, Pure Appl. Chem., 50 (1978) 1707.
28 H. Matsuura and M. Tasumi, in J.R. Durig (Ed.), Vibrational Spectra and Structure, V.12, Elsevier, Amsterdam, 1983, pp. 69–143.
29 B.L. Crawford, Jr. and W.H. Fletcher, J. Chem. Phys., 19 (1951) 141.
30 B.L. Crawford, Jr. and J. Overend, J. Mol. Spectrosc., 12 (1964) 307.
31 R.A. Kydd, Spectrochim. Acta, Part A, 27 (1971) 2067.
32 C.E. Sun, R.G. Parr, and B.L. Crawford, Jr., J. Chem. Phys., 17 (1949) 840.
33 G. Arfken, Mathematical Methods for Physicists, Academic, New York, 1970.
34 E.B. Wilson, Jr., J.C. Decius, and P.C. Cross, Molecular Vibrations, McGraw-Hill, New York, 1955.
35 C.M. Cook, Quantum Chem. Prog. Exchange Program 391, Indiana University, Bloomington, IN.
36 H.B. Schlegel, Quantum Chem. Prog. Exchange Program 427, Indiana University, Bloomington, IN.
37 Y. Xie and J.E. Boggs, J. Comput. Chem., 7 (1986) 158.
38 K. Fan and J.E. Boggs, J. Mol. Struct. (Theochem), 139 (1986) 283.
39 G. Zerbi, in A.J. Barnes and W.J. Orville-Thomas (Eds.), Vibrational Spectroscopy — Modern Trends, Elsevier, Amsterdam, 1977, pp. 261–284.
40 (a) E.R. Lippincott and R. Schroeder, J. Chem. Phys., 23 (1955) 1099.
(b) R. Schroeder and E.R. Lippincott, J. Phys. Chem., 61 (1957) 921.

41 A.L. Aljibury, R.G. Snyder, H.L. Strauss, and K. Raghavachari, J. Chem. Phys., 84 (1986) 6872.
42 H.B. Schlegel, S. Wolfe, and F. Bernardi, J. Chem. Phys., 63 (1975) 3632.
43 P. Pulay, J.G. Lee, and J.E. Boggs, J. Chem. Phys., 79 (1983) 3382.
44 W. Person and G. Zerbi (Eds.), Vibrational Intensities in Infrared and Raman Spectroscopy, Elsevier, Amsterdam, 1982.
45 R.G. Snyder, J. Chem. Phys., 42 (1965) 1744.
46 A.M. Dwivedi and S. Krimm, Macromolecules, 15 (1982) 177.
47 C. Destrade, E. Dupart, M. Joussot-Dubien, and C. Garrigou-Lagrange, Can. J. Chem., 52 (1974) 2590.
48 T. Shimanouchi, H. Matsuura, Y. Ogawa, and I. Harada, J. Phys. Chem. Ref. Data, 7 (1978) 1323.